Rainbow trout slow myoblast cell culture as a model to study slow skeletal muscle and the characterization of *mir-133* and *mir-499* families as a case study.

Bruno Oliveira da Silva Duran[1], Maeli Dal-Pai-Silva[1*], Daniel Garcia de la serrana[2,3]

[1]São Paulo State University (UNESP), Institute of Biosciences, Department of Morphology, Botucatu, São Paulo, Brazil

[2]University of St. Andrews, Scottish Oceans Institute, School of Biology, St. Andrews, Fife, Scotland, United Kingdom

[3]University of Barcelona, Faculty of Biology, Department of Cell Biology, Physiology and Immunology, Barcelona, Spain

*Corresponding Author

maeli.dal-pai@unesp.br

Keywords: Slow skeletal muscle; Cell culture; Myoblasts; miRNA; Electrostimulation.

Summary statement

Fish slow myoblast cell culture allows for the investigation of slow muscle physiology and comparative studies with fast muscle, such as *mir-133* and *mir-499* families in muscle development.

Abstract

Muscle fibers are classified as fast, intermediate and slow. *In vitro* myoblast cell culture model from fast muscle is a very useful tool to study muscle growth and development, however, similar models for slow muscle do not exist. Thanks to the compartmentalization of fish muscle fibers we developed a slow myoblast cell culture for rainbow trout (*Oncorhynchus mykiss*). Slow and fast muscle-derived myoblasts had similar morphology, but with differential expression of slow muscle markers such as *slow myhc, sox6* and *pgc-1α*. We also characterized the *mir-133* and *mir-499* microRNA families in trout slow and fast myoblasts as a case study during myogenesis and in response to electrostimulation. Three *mir-133* (*a-1a*, *a-1b* and *a-2*) and four *mir-499* (*aa*, *ab*, *ba* and *bb*) paralogues were identified for rainbow trout and named base on their phylogenetic relationship to zebrafish and Atlantic salmon orthologues. *Omy-mir-499ab* and *omy-mir-499bb* had 0.6 and 0.5-fold higher expression in slow myoblasts compared to fast myoblasts, whereas *mir-133* duplicates had similar levels in both phenotypes and little variation during development. Slow myoblasts also showed increased expression for *omy-mir-499b* paralogues in response to chronic electrostimulation (7-fold increase for *omy-mir-499ba* and 2.5-fold increase for *omy-mir-499bb*). The higher expression of *mir-499* paralogues in slow myoblasts suggests a role in phenotype determination while the lack of significant differences of *mir-133* copies during culture development might indicate a different role in fish compared to mammals. We have also found signs of sub-functionalization of *mir-499* paralogues after electrostimulation, with *omy-mir-499b* copies more responsive to electrical signals.

Introduction

Skeletal muscle is the most abundant tissue in teleost fish and can represent up to 60% of total body mass (Johnston, 2001). Skeletal muscle is key for fish propulsion, represents the biggest protein reservoir and is the main product of the aquaculture industry (Johnston, 2001; Sänger and Stoiber, 2001).

Muscle fiber types are classified based on their contractile and metabolic properties as fast, intermediate and slow (Johnston et al., 2004). Fast fibers comprise up to 80-90% of the skeletal muscle and are characterized by fast-twitch, predominant anaerobic metabolism, low concentrations of myoglobin, mitochondria content, lipids, and low capillary density. The fast fibers are recruited during intense activity, associated with food capture and escape behavior (Sänger and Stoiber, 2001). Slow fibers comprise 5-20% of muscle mass and are located along the fish body, with a thicker region on the lateral line. They are characterized by having slow-twitch, predominant aerobic metabolism, high levels of myoglobin, mitochondria content, lipids, and high capillary density (Sänger and Stoiber, 2001). Despite their relatively low abundance, the slow muscle is the main tissue involved in sustained swimming and critical for middle and long-distance migrations (Bone, 1978; Sänger and Stoiber, 2001). The intermediate fibers have intermediate contractile and metabolic properties between fast and slow fibers and lie physically located between these two compartments representing a very marginal proportion of the total skeletal muscle (Sänger and Stoiber, 2001).

Postembryonic skeletal muscle growth occurs through the activation of myogenic precursor cells (MPCs). MPCs are located between the basal lamina and the sarcolemma of the muscle fibers, and under the absence of stimuli they remain in a quiescent state (then known as satellite cells) (Hollway et al., 2007; Rossi and Messina, 2014; Seger et al., 2011). Satellite cells re-enter the cell cycle in response to different stimuli, such as growth factors, hormones, cytokines, injury, exercise and nutrition, becoming proliferative myoblasts that can either fuse to each other forming new fibers (hyperplasia) or fuse to pre-existent fibers contributing to their growth in size (hypertrophy) (Johnston, 2006; Johnston et al., 2011), a process globally known as myogenesis. The establishment of the fish fast myoblast cell culture model has helped to characterize the molecular networks controlling myogenesis (Bower and Johnston, 2010b; Garcia de la serrana and Johnston, 2013; Johnston et al., 2011). The *in vitro* model recapitulates the main stages of the myogenesis starting with round quiescent cells, followed by proliferative myoblasts and differentiating myotubes (Gabillard et al.,

Journal of Experimental Biology • Accepted manuscript

2010; Vélez et al., 2016). Myoblast cell culture facilitates the study of the molecular networks involved in muscle formation in response to specific inputs, such as growth factors and nutrition (Duran et al., 2015; Duran et al., 2019; Garcia de la serrana and Johnston, 2013; Johnston et al., 2011; Vélez et al., 2014). The compartmentalization of skeletal muscle in fish makes possible to isolate myoblasts from fast and slow muscle, something very difficult in mammals due to the mixture of fast and slow fibers (Schiaffino and Reggiani, 2011). Until now, the myoblast cell culture had been only developed for fast skeletal muscle, while a similar model for slow muscle was not established.

The teleost lineage has undergone a specific whole genome duplication (WGD) around 450-320 million years ago (Mya) (Jaillon et al., 2004). As a result, several signaling pathways and molecular networks have some of their components expanded with multiple paralogue copies. It has been estimated that around 15-21% of the duplicated paralogues originated during the WGD have been retained (Garcia de la serrana et al., 2014b). In addition, the salmonid lineage went through an additional WGD around 75 Mya with an estimated 50% paralogues retention (Macqueen and Johnston, 2014; Macqueen et al., 2010; Macqueen et al., 2013). Paralogue genes can be retained after a WGD through three main mechanisms: sub-functionalization (each paralogue retains part of the original function of the ancestral gene), neo-functionalization (paralogue acquires a different function from the ancestral gene) or redundancy (multiples copies of a gene confer some advantage) (Bower and Johnston, 2010a; Garcia de la serrana and Johnston, 2013; Garcia de la serrana et al., 2014b; Garcia de la serrana et al., 2017; Maere and Van de Peer, 2010).

There is also evidence of microRNA (miRNA) families expanded after the teleost WGD (Berthelot et al., 2014). The primary function of these types of small noncoding RNAs (ncRNA) is the post-transcriptional regulation of gene expression, promoted by translational inhibition and decay of target messenger RNAs (mRNAs) (Ge and Chen, 2011). MiRNAs play an orchestrated regulation of multiple targets, controlling several signaling pathways and biological functions (Goljanek-Whysall et al., 2012; van Rooij et al., 2008). Based on the high conservation observed in miRNAs among vertebrates, it can be anticipated that a considerable set of mRNAs are under the modulation by miRNAs in teleosts (Bizuayehu and Babiak, 2014). Some miRNAs such as *mir-1*, *mir-133*, *mir-206* and *mir-499* are specifically or highly expressed in cardiac and/or skeletal muscles, and are involved in myogenesis, myoblast proliferation, differentiation, fiber type specification and muscle regeneration (Chen et al., 2006; Ge and Chen, 2011; van Rooij et al., 2009). Previous studies in pacu (*Piaractus mesopotamicus*) showed that fast and slow muscles have different miRNA expression patterns, as was the case of *miR-499* that exhibited higher levels of transcription in slow muscle (Duran et al., 2015), suggesting its involvement in the specification and maintenance of slow-twitch phenotype as previously observed in mammals (McCarthy, 2011; van Rooij et al., 2009). In such a context, the innervation pattern has been suggested to be essential for muscle fiber type specification; a tonic and low-frequency neural stimulation induces the slow phenotype, whereas a phasic and high-frequency neural stimulation promotes the fast phenotype (Chin et al., 1998; Olson and Williams, 2000). In the past years, studies have shown that muscle fiber neural activation can be recreated by electrical pulse stimulation (EPS) of cultured skeletal muscle cells (Fujita et al., 2007; Marotta et al., 2004; Thelen et al., 1997). EPS models are useful to investigate adaptive responses of skeletal muscle cells to different patterns of contractile activity, for instance the study of molecular and cellular mechanisms during simulation of resistance training or endurance training (Burch et al., 2010; Nedachi et al., 2008; Nikolić et al., 2012; Silveira et al., 2006). Therefore, the electrostimulation represents an important tool to investigate the roles of molecules involved with the regulation of muscle growth and phenotype, such as the miRNAs.

In the present work, we established a slow muscle myoblast cell culture from rainbow trout (*Oncorhynchus mykiss*) (Cleveland and Weber, 2010; Gabillard et al., 2010; Montserrat et al., 2007a; Seiliez et al., 2008) and used it to characterize the *mir-133* and *mir-499* families during slow and fast myoblasts development and in response to EPS applied on slow muscle cell cultures.

Material and methods

<u>Ethics statement and animals</u>

All experiments and procedures were approved by the Animal Welfare and Ethics Committee (AWEC) of the University of St Andrews and were carried out in accordance with relevant guidelines and regulations. Rainbow trout (*Oncorhynchus mykiss*) juveniles (10-15g) were obtained from Frandy Farm (Gleneagles, Scotland) and transported to the Scottish Oceans Institute aquarium facilities (University of St Andrews). Animals were evenly distributed in duplicated 200L fiberglass tanks, maintained in a freshwater re-circulatory system at temperature between 12-15°C and fed *ad libitum* daily with commercial diet provided by the same farm of origin. Trouts were humanely killed by head dislocation followed by the destruction of the brain with a scalpel according to Schedule 1 protocols as described in the Animals (Scientific Procedures) Act 1986 (Home Office Code of Practice. HMSO: London January 1997).

Myoblast cell culture

A total of 4 independent myoblasts cell cultures were performed as previously described (Fauconneau and Paboeuf, 2000). Briefly, fast muscle samples were collected from the epaxial region and slow muscle was carefully dissected around the lateral line (n=14-16 fish per culture until reaching a total of 20 g per tissue). Fast and slow muscle were mechanically dissociated with scalpels and enzymatically digested with 0.2% type I collagenase (Sigma-Aldrich, USA) and 0.1% trypsin (Sigma-Aldrich, USA). Cells were filtered through 40 and 100µm cell strainers (Thermo Fischer Scientific, USA) to remove any debris. After several washes, cells were resuspended in DMEM media (Dulbecco's Modified Eagle's Medium, 9mM $NaHCO_3$, 20mM HEPES, pH 7.4 - Sigma-Aldrich, USA) with 10% fetal bovine serum (FBS) and 1% antibiotic mixture (Sigma-Aldrich, USA). After cell counting in a Neubauer chamber, cells were diluted to a final concentration of 2×10^6 cells/mL and seeded in poly-L-lysine and laminin pre-treated 6-wells plates. Slow and fast myoblasts were maintained at 18°C for a total period of 12 days. Culture media was changed daily, and myoblast morphology was regularly monitored using a Leica DM IL Inverted Microscope coupled with the Leica DFC320 Digital Camera system (Leica, Germany). Total RNA was extracted from cells at days 2, 4, 6, 8, 10 and/or 12.

Electrical pulse stimulation (EPS)

Electrostimulation was performed using a C-Pace EP Cell Culture Stimulator in conjunction with the C-Dish Electrode Assemblies (IonOptix, USA). Myoblasts were electro-stimulated daily from day 4 of culture until day 10 following three different protocols: control plate (CTR; non-treated cells), acute treatment (A-EPS; cells treated with acute and high-frequency stimulation, simulating fast muscle innervation) and chronic treatment (C-EPS; cells treated with chronic and low-frequency stimulation, simulating slow muscle innervation). The acute treatment was applied for 15 minutes and the myoblasts were submitted to pulse trains of 10Hz and 30V for 10ms, given every 5th second. The chronic treatment was applied for 2 hours and the myoblasts were submitted to pulse trains of 1Hz and 30V for 2ms. The myoblasts were electro-stimulated in serum-free DMEM media and remained resting for 10 minutes before adding fresh media. RNA extractions for days 6, 8 and 10 of cell culture were performed 2 hours after the EPS.

miRNA phylogenetic analysis

Initially, the precursor sequences of miRNAs *mir-133*, *mir-499* and *mir-206* (a miRNA also highly expressed in muscle (Ge and Chen, 2011; Ma et al., 2015)) were obtained from zebrafish (*Danio rerio*) genome using the Ensembl Genome Browser 89 (http://www.ensembl.org/index.html). Zebrafish miRNAs were used as query against the available rainbow trout genome in Genoscope (https://www.genoscope.cns.fr/trout/) (Berthelot et al., 2014). Identified trout orthologues were initially named as *omy-mir-133* and *omy-mir-499* until their identity was phylogenetically established. Orthologues for *mir-133* and *mir-499* precursor sequences (pre-miRNA) from different teleost (*Astyanax mexicanus*, *Danio rerio*, *Gasterosteus aculeatus*, *Oreochromis niloticus*, *Oryzias latipes*, *Takifugu rubripes*, *Tetraodon nigroviridis*) and mammals (*Homo sapiens*, *Mus musculus*, *Pan troglodytes*, *Rattus norvegicus*) were retrieved from the Ensembl database. In addition, pre-miRNA orthologues for Atlantic salmon (*Salmo salar*) and coho salmon (*Oncorhynchus kisutch*) were also obtained from SalmoBase (https://salmobase.org/) (Samy et al., 2017) and NCBI (http://www.ncbi.nlm.nih.gov). The pre-miRNA sequences (Supplementary File S1) were aligned using MAFFT version 7 (http://mafft.cbrc.jp/alignment/server/), while MEGA7 software (Kumar et al., 2016) was used to estimate the best evolutionary model from aligned sequences. Bayesian MCMC phylogenetic trees following a Yule speciation process model and UPGMA starting tree were generated for each alignment using BEAST v1.7.4 software (Drummond et al., 2012) with 10,000,000 seeds. Final Bayesian trees were generated using TreeAnnotator v.1.7 with a burning value of 1000. All trees were visualized and edited using FigTree v.1.4.2 (http://tree.bio.ed.ac.uk/software/figtree/).

RNA extraction and reverse transcription

Total RNA was extracted using TRIsure™ (Bioline Reagents, United Kingdom), according to the manufacturer's recommendations, and stored at -80ºC for further analysis. Total RNA was quantified by spectrophotometry using a Nanodrop (ND1000) (Thermo Scientific, USA) while integrity was evaluated by 1% ethidium bromide agarose gel electrophoresis. All samples had 280/260nm and 230/260nm ratios above 1.8, indicating high-quality RNA. A total of 224ng of total RNA per sample were reverse transcribed using the miScript II RT Kit and QuantiTec Reverse Transcription Kit (Qiagen, Germany), following the manufacturer's guidelines. The resulting cDNA was used for quantitative PCR (qPCR).

Primer design

Primers for rainbow trout *slow myosin heavy chain* (*smyhc*), *fast myosin heavy chain* (*fmyhc*), *sry sex determining region Y-box 6* (*sox6*) , *six homeobox 1* (*six1*), *insulin-responsive glucose transporter type 4* (*glut4*), *late endosomal/lysosomal adaptor, mapk and mtor activator 3* (*lamtor3*), *ras related GTP binding D* (*ragd*), *regulatory associated protein of mtor complex 1* (*rptor*), *muscle atrophy f-box protein* (*mafbx/fbxo32*), *peroxisome proliferator-activated receptor gamma coactivator 1 alpha* (*pgc-1α*), *creatine kinase, m-type a* (*ckma*), *creatine kinase, m-type b* (*ckmb*), *myogenin* (*myog*), *ribosomal protein L13* (*rpl13*), *ribosomal protein L19* (*rpl19*), paralogues of *omy-mir-133* (133a-1a, 133a-1b and 133a-2), *omy-mir-499* (499aa, 499ab, 499ba, 499bb), *omy-mir-206-1* and *U6 snRNA* (*U6 small nuclear RNA*) were designed using Primer3 v.0.4.0 (Koressaar and Remm, 2007; Untergasser et al., 2012) (Supplementary File S2). The precursor sequences from each rainbow trout miRNA were used to design the forward and reverse primers in regions with low similarity in order to amplify individual paralogues (primers for *omy-mir-499aa* amplified both *499aa* and *499ab* copies, resulting in a global *omy-mir-499a* expression (aa+ab). Primers for miRNA were designed to work at 60°C and amplify 60-100bp regions while primers for mRNA were designed to work at 60°C and amplify 50-200bp regions. Any possible hairpin, self-dimer or cross-dimer structures formed by the primer pairs were estimated using NetPrimer software (Premier Biosoft, USA).

Quantitative real time PCR (qPCR)

All qPCR performed were compliant with the Minimum Information for Publication of Quantitative Real Time PCR experiments (MIQE) guidelines (Bustin et al., 2009). Each qPCR reaction contained 6µL of diluted cDNA (1:40), 7.5µL of SensiFAST™ SYBR® master mix (Bioline Reagents, United Kingdom) and 1.5µL of 500nM forward/reverse primer mix. The reactions were performed in duplicates under the following conditions: one cycle at 95°C for 2 minutes followed by 40 cycles of denaturation at 95°C for 5 seconds and annealing/extension at 65°C for 20 seconds in a MX3005P Real Time PCR System (Agilent Technologies, USA). The specificity of each primer set was confirmed by the presence of a single-peak dissociation curve. Gene expression was estimated using the $2^{-\Delta\Delta Ct}$ method (Livak and Schmittgen, 2001). Different housekeeping genes were tested (*rpl13*, *rpl19*, *omy-mir-206-1* and *U6 snRNA*) and NormFinder software (Andersen et al., 2004) was used to identify the optimal normalization gene for miRNA and mRNA expression. *Rpl13* and *omy-mir-206-1* were identified as the most suitable housekeeping genes for mRNA and miRNA expression respectively. The secondary structure of the identified miRNA precursor sequences was predicted using the RNAfold WebServer (Gruber et al., 2008) (Supplementary File S3).

Statistical analysis

Statistical analyses were performed using RStudio v1.0.136 (RStudio Team, 2015) and statistical significance was set at 5% ($p<0.05$). The normalities of the expression data were tested using Shapiro-Wilk test. When normality assumption was fulfilled, data were analyzed using a two-way ANOVA followed by post hoc Tukey's honestly significant difference (HSD) test, with the tissue of origin (*tissue*) and the day of development (*development*) as factors. When normality assumption was not fulfilled, data were transformed using the Box-Cox power transformation approach (Box and Cox, 1964) and analyzed as described. In addition, miRNA expression data from slow and fast myoblasts comparison were analyzed using the unpaired t-test with *tissue* as factor, and miRNA expression data from EPS treatments were analyzed using a one-way ANOVA followed by post hoc Dunn's test, with *treatment* as factor for the analysis. Pearson's correlation was used to access interesting relationships between evaluated genes. All graphs were constructed using ggplot2 R package (Wickham, 2016).

Results

Myoblast cell culture

Fast myoblast cell culture requires small juveniles (3-5g) in order to maximize the number of myoblasts obtained (Castillo et al., 2002; Castillo et al., 2006; Garcia de la serrana and Johnston, 2013; Montserrat et al., 2007b). However, slow muscle extraction requires bigger animals in order to be able to discriminate between tissues and dissect pure slow muscle. We found that rainbow trout around 15g of body weight yield enough fast and slow myoblasts from individual animals to perform the experiment described in the present study (Fig. 1A). Compared to fast skeletal muscle, slow muscle extraction requires a harder mechanical dissociation, does not change DMEM color (lactate from fast muscle turn it orange) and originates a top layer of fat that if not removed would reduce the efficiency of extraction (Fig. 1B, black arrow). At the end of the extraction protocol, slow skeletal muscle consistently yielded more cells per gram of tissue than fast skeletal muscle (data not shown). Slow and fast myoblasts were morphologically very similar with equivalent developmental stages during the culture progression: round mononucleated cells between days 1 and 2, proliferative myoblasts between days 3-7 and distinctive myotubes between days 8-12 (Fig. 1C, white arrows).

Characterization of slow muscle-derived myoblast cell culture

Myogenic nature of the cell cultures was confirmed by the expression of the muscle specific transcription factor *myogenin* (*myog*) during the myotube formation phase (Supplementary File S4) (Johnston, 2006). Slow-derived myoblasts phenotype was confirmed by analyzing the expression of *smyhc, fmyhc, six1* and *sox6* during the culture progression (Fig. 2). Expression of *fmyhc* and *smhyc* was significantly different between cell cultures (*tissue* $P<0.001$ and *development* $P<0.001$) (Fig. 2A-B). The *fmyhc* abundance was 2.5-fold higher in fast muscle cell culture between days 8 and 12 (Fig. 2B) while *smyhc* showed a >12-fold increase in slow muscle myotubes (Fig. 2A). The *six1* and *sox6* transcription factors expression levels were higher in fast than slow myoblast cell culture (*tissue* $P<0.001$ for both genes) (Fig. 2C-D). Both transcription factors had maximal abundance between days 6 to 10 (*development* $P<0.001$ for both genes) (Fig. 2C-D).

In order to investigate metabolic differences between tissues, we studied the expression of genes related to protein balance (*lamtor3*, *ragd*, *rptor* and *mafbx*), glucose uptake (*glut4*) and energy (*pgc1α*, *ckma* and *ckmb*) (Fig. 3). Despite differences between slow and fast muscle cells were not significant for *glut4*, *lamtor3* and *ragd* (*tissue* P=0.58, P=0.22 and P=0.63 respectively) (Fig. 3A-C), their transcription was slightly higher on slow cell culture and decreased between days 8 to 12 (Fig. 3A and C). In both tissues, the *mafbx* expression similarly (*tissue* P=0.05) decreased suddenly after day 2 (*development* P<0.001) and remained low until the end of the culture, while *rptor* did not change between tissues (*tissue* P=0.53) or culture development (*development* P=0.07) (Fig. 3D-E). In contrast, *pgc1α* expression was stable during the cell culture (*development* P=0.59) and significantly higher in slow culture (*tissue* P<0.001) (Fig. 3F). The expression pattern of *ckma* and *ckmb* paralogues was very similar between slow and fast muscle cells (*tissue* P=0.28 for *ckma* and P=0.36 for *ckmb*), with maximal expression during myotube formation (days 8 to 12) (*development* P<0.001 for both genes) (Fig. 3G-H).

miRNA identification

Several members of the *mir-133* and *mir-499* families were identified for rainbow trout, coho and Atlantic salmon. We used phylogenetic analysis to establish their identity and name them based on the existent zebrafish and salmonid nomenclature. Phylogenetic analysis confirmed the existence of three copies of *mir-133* (Fig. 4) and four of *mir-499* (Fig. 5) in rainbow trout. According to the tree topology, rainbow trout paralogues were named as *omy-mir-133a-1a*, *omy-mir-133a-1b*, *omy-mir-133a-2*, *omy-mir-499aa*, *omy-mir-499ab*, *omy-mir-499ba* and *omy-mir-499bb* (Fig. 4 and 5; Supplementary File S1). Globally, miRNA sequences were very conserved, with identities over 92% (Supplementary File S5). We also observed that paralogues of the same family had very similar secondary structures while differences between *mir-133* and *mir-499* families were also clear (Supplementary File S3). Due to the high degree of identity, the primers designed for *omy-mir-499aa* also amplified the *omy-mir-499ab* copy, and therefore *omy-mir-499aa* paralogue represents the sum of both (*omy-mir-499aa+ab*).

miRNA expression during fast and slow myoblast culture development

Expression of *mir-133* and *mir-499* paralogues was studied in slow and fast-derived myoblast cell cultures at days 6, 8 and 10 of development (Fig. 6). No significant differences in expression were found for any of the *omy-mir-133* paralogues between slow and fast cell cultures (Fig. 6A-C). Between days 6 to 8, expression was 0.5-fold lower for *omy-mir-499aa+ab* and *omy-mir-499bb* and 0.6-fold lower for *omy-mir-499ab* in fast compared to slow-derived myocytes (*tissue* $P<0.01$) (Fig. 6D-G). *Omy-mir-499* copies did not show statistical differences during culture development (*development* $P=0.62$, $P=0.88$, $P=0.86$ and $P=0.94$ for *omy-mir-499aa+ab*, *omy-mir-499ab*, *omy-mir-499ba* and *omy-mir-499bb* respectively) (Fig. 6D-G).

Expression of *omy-mir-133* and *omy-mir-499* paralogues in response to electrical stimulation on slow muscle myoblasts were also investigated (Fig. 7). From the *omy-mir-133* family, only *omy-mir-133a-2* transcription significantly increased by 2-fold at day 6 of chronic stimulation (C-EPS group) (*treatment* $P<0.05$) (Fig. 7A-C). The expression of *omy-mir-499ab* at day 6 was 0.5-fold lower in C-EPS treated cells than the CTR group (*treatment* $P<0.05$) (Fig. 7E). *Omy-mir-499ba* transcription was 7-fold higher at day 6 and 4-fold higher at day 8 (*treatment* $P<0.001$) in C-EPS treated cells compared to CTR group (Fig. 7F). The chronic stimulation also increased expression of *omy-mir-499bb* paralogue, by 2.5-fold at day 6 (*treatment* $P<0.001$) and by 2-fold at day 8 (*treatment* $P<0.01$). Besides, *omy-mir-499bb* expression at day 6 was 2.3-fold higher in acute-stimulated myoblasts (A-EPS group) compared to CTR group (*treatment* $P<0.01$) (Fig. 7G).

To complement our results and provide further insight into miRNA paralogue roles, we performed correlation analyses between expression of *omy-mir-133*, *omy-mir-499*, *smyhc*, *fmyhc* and *sox6* (Supplementary File S6). It is interesting to highlight the negative correlation between *omy-mir-499* paralogues and *sox6* ($\rho=-0.38$ for *omy-mir-499aa+ab* vs *sox6*; $\rho=-0.5$ for *omy-mir-499ba* vs *sox6*; $\rho=-0.51$ for *omy-mir-499bb* vs *sox6*) all of them significant (Supplementary File S6).

Discussion

In the present study, we established a viable teleost slow myoblast cell culture, similar to the fast myoblast cell culture with some considerations: 1) the slow muscle is much firmer and very easy to lose during washes; 2) a layer of fat is formed during extraction that should be removed in order to increase cell yield; 3) after enzymatic digestion slow muscle is especially rich in tissue debris and should be thoughtfully filtered and washed; and 4) for an equivalent amount of tissue, slow muscle yield 43% more myoblasts than fast muscle (based on Neubauer chamber counting; data not shown). Unless the experimental design requires samples from the same animals, we recommend using small juveniles to extract fast and bigger animals for slow skeletal muscle. The difference in the number of myoblasts extracted from both tissues is in agreement with previous studies reporting higher proportion of satellite cells in slow fibers (Gibson and Schultz, 1982) but with equivalent development stages as described for fast myoblasts cell cultures (Fig. 1) (Bower and Johnston, 2010a; Castillo et al., 2006; Garcia de la serrana et al., 2014a).

Despite the morphological similarities between the slow and fast muscle cells, they were phenotypically different, as indicated by the expression profiles of *six1*, *sox6*, *fmyhc* and *smyhc*. Sox6 is a transcription factor that represses slow fibers phenotype (Hagiwara et al., 2007), while Six1, another transcription factor, is required for the determination of the fast phenotype (Bessarab et al., 2008). Our results show that *six1* and *sox6* levels were significantly lower in slow myogenic cells, indicating that the slow program was not repressed (Fig. 2). Slow myogenic cells had a much higher expression of *smyhc* compared to *fmyhc* (Fig. 2). Our results suggest that myoblasts from slow and fast muscle tend to differentiate to the fiber type of the tissue they were extracted from, in agreement with previous studies on birds, where myoblasts extracted from pectoralis major and anterior latissimus dorsi formed fast and slow myotubes in a similar proportions as found in the muscle of origin (Feldman and Stockdale, 1991). It is interesting to note that slow muscle myogenic cells showed unexpectedly high levels of *fmyhc* (Fig. 2), raising questions about the possibility of some degree of phenotypic plasticity and turn into fast phenotype in response to endocrine, nutritional or electrical signals.

We analyzed the expression of genes involved in different metabolic processes in order to get a preliminary idea of the metabolic differences or similarities between slow and fast myoblasts. Many of the genes studied had a higher expression in the slow myoblasts (*glut4*, *lamtor3*, *ragd* and *pgc1α*), despite only *pgc1α* were statistically significant (Fig. 3). Pgc1α acts as co-factor of mitochondrial biogenesis, and it is crucial to maintain slow muscle oxidative metabolism (Chan and Arany, 2014). Moreover, slow fibers might be significantly more insulin-responsive than fast fibers, due to higher levels of Glut4 protein (Kern et al., 1990), as inferred by a higher transcription of *glut4* on slow myoblasts. Lamtor/Rrag GTPases complex has been identified to act as amino acid sensor and promote Mtor activation, representing an important mechanism through amino acids stimulate protein synthesis by themselves (Demetriades et al., 2014; Sancak et al., 2010). Despite the similar expression pattern of *rptor* between fast and slow cultures, *lamtor3* and *ragd* had higher transcription in slow myogenic cells (Fig. 3), suggesting a higher contribution of Lamtor/Rrag GTPases complex to protein synthesis. The idea of an increase in protein synthesis during the progression of the cell culture is further supported by the strong inhibition of *mafbx* expression, E3 ubiquitin ligase that regulates protein degradation, found in both tissues (Fig. 3) (Sandri, 2008).

We also used slow and fast muscle cell cultures as a model to characterize *mir-133* and *mir-499* families during differentiation and in response to electrostimulation. The miRNA mature sequences and secondary structures are highly conserved among different vertebrate species and between paralogues of the same family (Bizuayehu and Babiak, 2014). Phylogenetic analysis confirmed the identity of three *mir-133* (*omy-mir-133a-1a*, *omy-mir-133a-1b* and *omy-mir-133a-2*) and four *mir-499* (*omy-mir-499aa*, *omy-mir-499ab*, *omy-mir-499ba* and *omy-mir-499bb*) in rainbow trout, as expected after successive WGD. It is also interesting to highlight that rainbow trout seems to lack *mir-133b* and *-133c*, indicating a species-specific lost.

The *omy-mir-133* paralogues had similar levels of expression between fast and slow myoblast cell cultures with very little variation during development (Fig. 6). The *mir-133* has been described to be involved in muscle development by preventing myoblast differentiation and enhancing myoblast proliferation (Chen et al., 2006; Yu et al., 2014) what disagrees with the lack of transcriptional variation found in our study. Due to *mir-133* levels were unaffected in almost all conditions, expression of the target *srf* (*serum responsive factor*) was not determined in the present study. It might be possible that *mir-133* has a different role in fish than suggested in mammals, or that relevant changes occurred before day 6 of development, not included in the present work and that would need further investigation.

The *omy-mir-499* paralogues had higher abundance in slow myoblasts (Fig. 6), which is in agreement with the role of this miRNA promoting slow fiber type phenotype (van Rooij et al., 2009; Wang et al., 2011). Both in mammals (McCarthy et al., 2009; van Rooij et al., 2009) and teleost fish (Duran et al., 2015; Nachtigall et al., 2015; Wang et al., 2011), *miR-499* mediates the translational repression of *sox6*, a putative target involved in the maintenance of the fast-twitch phenotype through the repression of slow-twitch-specific genes, such as *slow myosin heavy chain 1* (von Hofsten et al., 2008). Our results show a negative correlation between several *omy-mir-499* paralogues and *sox6*, suggesting that a similar mechanism might be in place in slow myoblasts cell culture. These data are corroborated by the positive correlation between *omy-mir-499ab* and *smyhc*, as opposite to *omy-mir-499bb* and *fmyhc* (Supplementary File S6). In response to electrical stimulation both *mir-499b* paralogues (*omy-mir-499ba* and *omy-mir-499bb*) increased their transcription after C-EPS treatment indicating that *mir-499b* paralogues could be more susceptible to long-term electrical stimuli than *mir-499a* duplicates. Results from the C-EPS treatment suggest that the *mir-499b* paralogues might have an active role in slow fiber type specification and maintenance. However, considering the decreased expression of *omy-mir-499ab* at day 6 and a tendency of increased expression of *omy-mir-499aa+ab* at day 10 in C-EPS myoblasts (Fig. 7), another possibility could be that *omy-mir-499b* paralogues have an early role in slow phenotype determination, while *omy-mir-499a* copies may act in the late stage of myotube formation. Both possibilities suggest the sub-functionalization of *omy-mir-499* paralogues, as a result of the teleost-specific WGD (Jaillon et al., 2004). Our study shows that *omy-mir-499b* paralogues probably retained only part of the original function of the *omy-mir-499* gene, appearing to be more responsive to electrical signals and/or more involved to phenotype specification at early stages compared to *omy-mir-499a* copies. Evidence of *myod1* (*myogenic differentiation factor 1*) paralogues sub-functionalization were also observed during myotube formation of Atlantic salmon muscle cells, with *myod1a* primarily expressed during cell differentiation and *myod1b* and *1c* especially expressed during cell proliferation (Bower and Johnston, 2010a). Given the increased expression of *mir-499b* copies in C-EPS group, we can conclude that chronic and slow-frequency stimulation enhanced the slow phenotype in cell culture and could be used in skeletal muscle fiber type studies.

The slow myoblast cell culture represents an interesting and useful *in vitro* model to the study of skeletal muscle. Particularities in processes such as muscle development, wasting and regeneration can be addressed in this system, in addition to modulation of muscle fiber phenotypes, such as studies investigating exercise and phenotypic plasticity. The cultured slow myoblasts offer the possibility for future manipulative and pharmacological experiments, including gain or loss of function assays that may provide new information about the roles of individual genes or signaling molecules. The next steps in the characterization of *mir-133* and *mir-499* paralogues in rainbow trout include the use of miRNA inhibitors and mimics to alter their expression and better define their function, which will increase the understanding of how these families regulate fish myogenesis.

Conclusions

We have successfully established a slow myoblast cell culture. The extraction of slow myoblasts opens the doors to future comparative studies between slow and fast muscle development, regulation and to study the physiology of the slow muscle. We have also characterized the members of the *mir-133* and *mir-499* family in rainbow trout and their expression profiles during myogenesis, confirming the role of *mir-499* on slow muscle phenotype determination and casting doubts about *mir-133* role during differentiation. In addition, we have found signs of sub-functionalization of *mir-499* paralogues in response to electrostimulation.

Acknowledgments

We will like to thank Professor Ian Alistair Johnston from the Scottish Oceans Institute (University of St Andrews) to host the present research in his laboratory facilities. We also thank Dr. Robson Francisco Carvalho and Dr. Edson Assunção Mareco for their valuable discussions.

Competing interests

No competing interests declared.

Funding

This work received funding from the MASTS pooling initiative (The Marine Alliance for Science and Technology for Scotland) and their support is gratefully acknowledged. MASTS is funded by the Scottish Funding Council (grant reference HR09011) and contributing institutions. Funding was also provided by the Coordination for the Improvement of Higher Education Personnel (CAPES), National Council for Scientific and Technological Development (CNPq), with grants 447233/2014 and 302656/2015-4, and São Paulo Research Foundation (FAPESP), with grants #2015/03234-8, #2016/19683-9 and #2016/05009-4. The funding agencies did not have roles in the design of the study, analysis of data or writing of manuscript, providing only the financial resources. DG is a Serra Húnter Tenure-Track Lecturer of the University of Barcelona.

Data availability

All data generated during this study are included in this published article. The datasets analyzed for this study can be found in the Ensembl Genome Browser 89 (http://www.ensembl.org/index.html), rainbow trout genome (https://www.genoscope.cns.fr/trout/) (Berthelot et al., 2014), SalmoBase (https://salmobase.org/) (Samy et al., 2017) and NCBI (http://www.ncbi.nlm.nih.gov).

Author contributions statement

BD, MS and DG conceived and designed the experiments. BD and DG performed the experiments. BD, MS and DG analyzed the data. MS and DG contributed with reagents/materials/analysis tools. BD, MS and DG wrote the paper. All authors read and approved the final manuscript.

References

Andersen, C. L., Jensen, J. L. and Ørntoft, T. F. (2004). Normalization of Real-Time Quantitative Reverse Transcription-PCR Data: A Model-Based Variance Estimation Approach to Identify Genes Suited for Normalization, Applied to Bladder and Colon Cancer Data Sets. *Cancer Res.* **64**, 5245–5250.

Berthelot, C., Brunet, F., Chalopin, D., Juanchich, A., Bernard, M., Noël, B., Bento, P., Da Silva, C., Labadie, K., Alberti, A., et al. (2014). The rainbow trout genome provides novel insights into evolution after whole-genome duplication in vertebrates. *Nat. Commun.* **5**, 3657.

Bessarab, D. A., Chong, S.-W., Srinivas, B. P. and Korzh, V. (2008). Six1a is required for the onset of fast muscle differentiation in zebrafish. *Dev. Biol.* **323**, 216–228.

Bizuayehu, T. T. and Babiak, I. (2014). MicroRNA in Teleost Fish. *Genome Biol. Evol.* **6**, 1911–1937.

Bone, Q. (1978). Locomotor muscle. In *Fish Physiology, Vol VII, Locomotion* (ed. Hoar, W.) and Randall, D.), p. 576. London: Academic Press, Inc.

Bower, N. I. and Johnston, I. A. (2010a). Paralogs of Atlantic salmon myoblast determination factor genes are distinctly regulated in proliferating and differentiating myogenic cells. *AJP Regul. Integr. Comp. Physiol.* **298**, R1615–R1626.

Bower, N. I. and Johnston, I. A. (2010b). Transcriptional Regulation of the IGF Signaling Pathway by Amino Acids and Insulin-Like Growth Factors during Myogenesis in Atlantic Salmon. *PLoS One* **5**, e11100.

Box, G. E. P. and Cox, D. R. (1964). An Analysis of Transformations. *J. R. Stat. Soc. Ser. B* **26**, 211–252.

Burch, N., Arnold, A.-S., Item, F., Summermatter, S., Brochmann Santana Santos, G., Christe, M., Boutellier, U., Toigo, M. and Handschin, C. (2010). Electric Pulse Stimulation of Cultured Murine Muscle Cells Reproduces Gene Expression Changes of Trained Mouse Muscle. *PLoS One* **5**, e10970.

Bustin, S. A., Benes, V., Garson, J. A., Hellemans, J., Huggett, J., Kubista, M., Mueller, R., Nolan, T., Pfaffl, M. W., Shipley, G. L., et al. (2009). The MIQE Guidelines: Minimum Information for Publication of Quantitative Real-Time PCR Experiments. *Clin. Chem.* **55**, 611–622.

Castillo, J., Le Bail, P.-Y., Paboeuf, G., Navarro, I., Weil, C., Fauconneau, B. and Gutiérrez, J. (2002). IGF-I binding in primary culture of muscle cells of rainbow trout: changes during in vitro development. *Am. J. Physiol. Integr. Comp. Physiol.* **283**, R647–R652.

Castillo, J., Ammendrup-Johnsen, I., Codina, M., Navarro, I. and Gutiérrez, J. (2006). IGF-I and insulin receptor signal transduction in trout muscle cells. *Am. J. Physiol. Integr. Comp. Physiol.* **290**, R1683–R1690.

Chan, M. C. and Arany, Z. (2014). The many roles of PGC-1α in muscle--recent developments. *Metabolism.* **63**, 441–51.

Chen, J.-F., Mandel, E. M., Thomson, J. M., Wu, Q., Callis, T. E., Hammond, S. M., Conlon, F. L. and Wang, D.-Z. (2006). The role of microRNA-1 and microRNA-133 in skeletal muscle proliferation and differentiation. *Nat. Genet.* **38**, 228–33.

Chin, E. R., Olson, E. N., Richardson, J. A., Yang, Q., Humphries, C., Shelton, J. M., Wu, H., Zhu, W., Bassel-Duby, R. and Williams, R. S. (1998). A calcineurin-dependent transcriptional pathway controls skeletal muscle fiber type. *Genes Dev.* **12**, 2499–509.

Cleveland, B. M. and Weber, G. M. (2010). Effects of insulin-like growth factor-I, insulin, and leucine on protein turnover and ubiquitin ligase expression in rainbow trout primary myocytes. *Am. J. Physiol. Integr. Comp. Physiol.* **298**, R341–R350.

Demetriades, C., Doumpas, N. and Teleman, A. A. (2014). Regulation of TORC1 in Response to Amino Acid Starvation via Lysosomal Recruitment of TSC2. *Cell* **156**, 786–799.

Drummond, A. J., Suchard, M. A., Xie, D. and Rambaut, A. (2012). Bayesian Phylogenetics with BEAUti and the BEAST 1.7. *Mol. Biol. Evol.* **29**, 1969–1973.

Duran, B. O. da S., Fernandez, G. J., Mareco, E. A., Moraes, L. N., Salomão, R. A. S., Gutierrez de Paula, T., Santos, V. B., Carvalho, R. F. and Dal-Pai-Silva, M. (2015). Differential microRNA Expression in Fast- and Slow-Twitch Skeletal Muscle of *Piaractus mesopotamicus* during Growth. *PLoS One* **10**, e0141967.

Duran, B. O. S., Góes, G. A., Zanella, B. T. T., Freire, P. P., Valente, J. S., Salomão, R. A. S., Fernandes, A., Mareco, E. A., Carvalho, R. F. and Dal-Pai-Silva, M. (2019). Ascorbic acid stimulates the in vitro myoblast proliferation and migration of pacu (*Piaractus mesopotamicus*). *Sci. Rep.* **9**, 2229.

Fauconneau, B. and Paboeuf, G. (2000). Effect of fasting and refeeding on in vitro muscle cell proliferation in rainbow trout (*Oncorhynchus mykiss*). *Cell Tissue Res.* **301**, 459–63.

Feldman, J. L. and Stockdale, F. E. (1991). Skeletal muscle satellite cell diversity: satellite cells form fibers of different types in cell culture. *Dev. Biol.* **143**, 320–34.

Fujita, H., Nedachi, T. and Kanzaki, M. (2007). Accelerated de novo sarcomere assembly by electric pulse stimulation in C2C12 myotubes. *Exp. Cell Res.* **313**, 1853–1865.

Gabillard, J. C., Sabin, N. and Paboeuf, G. (2010). In vitro characterization of proliferation and differentiation of trout satellite cells. *Cell Tissue Res.* **342**, 471–7.

Garcia de la serrana, D. and Johnston, I. A. (2013). Expression of Heat Shock Protein (Hsp90) Paralogues Is Regulated by Amino Acids in Skeletal Muscle of Atlantic Salmon. *PLoS One* **8**, e74295.

Garcia de la serrana, D., Codina, M., Capilla, E., Jiménez-Amilburu, V., Navarro, I., Du, S.-J., Johnston, I. A. and Gutiérrez, J. (2014a). Characterisation and expression of myogenesis regulatory factors during in vitro myoblast development and in vivo fasting in the gilthead sea bream (*Sparus aurata*). *Comp. Biochem. Physiol. Part A Mol. Integr. Physiol.* **167**, 90–99.

Garcia de la serrana, D., Mareco, E. A. and Johnston, I. A. (2014b). Systematic Variation in the Pattern of Gene Paralog Retention between the Teleost Superorders Ostariophysi and Acanthopterygii. *Genome Biol. Evol.* **6**, 981–987.

Garcia de la serrana, D., Fuentes, E. N., Martin, S. A. M., Johnston, I. A. and Macqueen, D. J. (2017). Divergent regulation of insulin-like growth factor binding protein genes in cultured Atlantic salmon myotubes under different models of catabolism and anabolism. *Gen. Comp. Endocrinol.* **247**, 53–65.

Ge, Y. and Chen, J. (2011). MicroRNAs in skeletal myogenesis. *Cell Cycle* **10**, 441–448.

Gibson, M. C. and Schultz, E. (1982). The distribution of satellite cells and their relationship to specific fiber types in soleus and extensor digitorum longus muscles. *Anat. Rec.* **202**, 329–337.

Goljanek-Whysall, K., Sweetman, D. and Münsterberg, A. E. (2012). microRNAs in skeletal muscle differentiation and disease. *Clin. Sci.* **123**, 611–625.

Gruber, A. R., Lorenz, R., Bernhart, S. H., Neuböck, R. and Hofacker, I. L. (2008). The Vienna RNA websuite. *Nucleic Acids Res.* **36**, W70–4.

Hagiwara, N., Yeh, M. and Liu, A. (2007). Sox6 is required for normal fiber type differentiation of fetal skeletal muscle in mice. *Dev. Dyn.* **236**, 2062–2076.

Hollway, G. E., Bryson-Richardson, R. J., Berger, S., Cole, N. J., Hall, T. E. and Currie, P. D. (2007). Whole-Somite Rotation Generates Muscle Progenitor Cell Compartments in the Developing Zebrafish Embryo. *Dev. Cell* **12**, 207–219.

Jaillon, O., Aury, J.-M., Brunet, F., Petit, J.-L., Stange-Thomann, N., Mauceli, E., Bouneau, L., Fischer, C., Ozouf-Costaz, C., Bernot, A., et al. (2004). Genome duplication in the teleost fish Tetraodon nigroviridis reveals the early vertebrate proto-karyotype. *Nature* **431**, 946–957.

Johnston, I. A. (2001). Genetic and Environmental Determinants of Muscle Growth Patterns. In *Muscle development and growth*, pp. 141–186. San Diego: Academic Press.

Johnston, I. A. (2006). Environment and plasticity of myogenesis in teleost fish. *J. Exp. Biol.* **209**, 2249–2264.

Johnston, I. A., Abercromby, M., Vieira, V. L. A., Sigursteindóttir, R. J., Kristjánsson, B. K., Sibthorpe, D. and Skúlason, S. (2004). Rapid evolution of muscle fibre number in post-glacial populations of Arctic charr Salvelinus alpinus. *J. Exp. Biol.* **207**, 4343–4360.

Johnston, I. A., Bower, N. I. and Macqueen, D. J. (2011). Growth and the regulation of myotomal muscle mass in teleost fish. *J. Exp. Biol.* **214**, 1617–28.

Kern, M., Wells, J. A., Stephens, J. M., Elton, C. W., Friedman, J. E., Tapscott, E. B., Pekala, P. H. and Dohm, G. L. (1990). Insulin responsiveness in skeletal muscle is determined by glucose transporter (Glut4) protein level. *Biochem. J.* **270**, 397–400.

Koressaar, T. and Remm, M. (2007). Enhancements and modifications of primer design program Primer3. *Bioinformatics* **23**, 1289–1291.

Kumar, S., Stecher, G. and Tamura, K. (2016). MEGA7: Molecular Evolutionary Genetics Analysis Version 7.0 for Bigger Datasets. *Mol. Biol. Evol.* **33**, 1870–1874.

Livak, K. J. and Schmittgen, T. D. (2001). Analysis of relative gene expression data using real-time quantitative PCR and the $2^{-\Delta\Delta Ct}$ Method. *Methods* **25**, 402–8.

Ma, G., Wang, Y., Li, Y., Cui, L., Zhao, Y., Zhao, B. and Li, K. (2015). MiR-206, a key modulator of skeletal muscle development and disease. *Int. J. Biol. Sci.* **11**, 345–52.

Macqueen, D. J. and Johnston, I. A. (2014). A well-constrained estimate for the timing of the salmonid whole genome duplication reveals major decoupling from species diversification. *Proceedings. Biol. Sci.* **281**, 20132881.

Macqueen, D. J., Kristjánsson, B. K. and Johnston, I. A. (2010). Salmonid genomes have a remarkably expanded akirin family, coexpressed with genes from conserved pathways governing skeletal muscle growth and catabolism. *Physiol. Genomics* **42**, 134–48.

Macqueen, D. J., Garcia de la serrana, D. and Johnston, I. A. (2013). Evolution of Ancient Functions in the Vertebrate Insulin-Like Growth Factor System Uncovered by Study of Duplicated Salmonid Fish Genomes. *Mol. Biol. Evol.* **30**, 1060–1076.

Maere, S. and Van de Peer, Y. (2010). Duplicate Retention After Small- and Large-Scale Duplications. In *Evolution after Gene Duplication* (ed. Dittmar, K.) and Liberles, D.), p. 329. Hoboken, NJ, USA: John Wiley & Sons, Inc.

Marotta, M., Bragós, R. and Gómez-Foix, A. M. (2004). Design and performance of an electrical stimulator for long-term contraction of cultured muscle cells. *Biotechniques* **36**, 68–73.

McCarthy, J. J. (2011). The MyomiR network in skeletal muscle plasticity. *Exerc. Sport Sci. Rev.* **39**, 150–4.

McCarthy, J. J., Esser, K. A., Peterson, C. A. and Dupont-Versteegden, E. E. (2009). Evidence of MyomiR network regulation of β-myosin heavy chain gene expression during skeletal muscle atrophy. *Physiol. Genomics* **39**, 219–226.

Montserrat, N., Gabillard, J. C., Capilla, E., Navarro, M. I. and Gutiérrez, J. (2007a). Role of insulin, insulin-like growth factors, and muscle regulatory factors in the compensatory growth of the trout (*Oncorhynchus mykiss*). *Gen. Comp. Endocrinol.* **150**, 462–472.

Montserrat, N., Sánchez-Gurmaches, J., García de la Serrana, D., Navarro, M. I. and Gutiérrez, J. (2007b). IGF-I binding and receptor signal transduction in primary cell culture of muscle cells of gilthead sea bream: changes throughout in vitro development. *Cell Tissue Res.* **330**, 503–513.

Nachtigall, P. G., Dias, M. C., Carvalho, R. F., Martins, C. and Pinhal, D. (2015). MicroRNA-499 expression distinctively correlates to target genes sox6 and rod1 profiles to resolve the skeletal muscle phenotype in Nile tilapia. *PLoS One* **10**, e0119804.

Nedachi, T., Fujita, H. and Kanzaki, M. (2008). Contractile C_2C_{12} myotube model for studying exercise-inducible responses in skeletal muscle. *Am. J. Physiol. Metab.* **295**, E1191–E1204.

Nikolić, N., Skaret Bakke, S., Tranheim Kase, E., Rudberg, I., Flo Halle, I., Rustan, A. C., Thoresen, G. H. and Aas, V. (2012). Electrical Pulse Stimulation of Cultured Human Skeletal Muscle Cells as an In Vitro Model of Exercise. *PLoS One* **7**, e33203.

Olson, E. N. and Williams, R. S. (2000). Calcineurin Signaling and Muscle Remodeling. *Cell* **101**, 689–692.

Rossi, G. and Messina, G. (2014). Comparative myogenesis in teleosts and mammals. *Cell. Mol. Life Sci.* **71**, 3081–3099.

RStudio Team (2015). RStudio: Integrated Development for R. *RStudio, Inc., Boston, MA.*

Samy, J. K. A., Mulugeta, T. D., Nome, T., Sandve, S. R., Grammes, F., Kent, M. P., Lien, S. and Våge, D. I. (2017). SalmoBase: an integrated molecular data resource for Salmonid species. *BMC Genomics* **18**, 482.

Sancak, Y., Bar-Peled, L., Zoncu, R., Markhard, A. L., Nada, S. and Sabatini, D. M. (2010). Ragulator-Rag Complex Targets mTORC1 to the Lysosomal Surface and Is Necessary for Its Activation by Amino Acids. *Cell* **141**, 290–303.

Sandri, M. (2008). Signaling in Muscle Atrophy and Hypertrophy. *Physiology* **23**, 160–170.

Sänger, A. M. and Stoiber, W. (2001). Muscle fiber diversity and plasticity. In *Muscle development and growth* (ed. Johnston, I. A.), pp. 187–250. San Diego: Academic Press.

Schiaffino, S. and Reggiani, C. (2011). Fiber Types in Mammalian Skeletal Muscles. *Physiol. Rev.* **91**, 1447–1531.

Seger, C., Hargrave, M., Wang, X., Chai, R. J., Elworthy, S. and Ingham, P. W. (2011). Analysis of Pax7 expressing myogenic cells in zebrafish muscle development, injury, and models of disease. *Dev. Dyn.* **240**, 2440–2451.

Seiliez, I., Gabillard, J.-C., Skiba-Cassy, S., Garcia-Serrana, D., Gutierrez, J., Kaushik, S., Panserat, S. and Tesseraud, S. (2008). An in vivo and in vitro assessment of TOR signaling cascade in rainbow trout (*Oncorhynchus mykiss*). *AJP Regul. Integr. Comp. Physiol.* **295**, R329–R335.

Silveira, L. R., Pilegaard, H., Kusuhara, K., Curi, R. and Hellsten, Y. (2006). The contraction induced increase in gene expression of peroxisome proliferator-activated receptor (PPAR)-γ coactivator 1α (PGC-1α), mitochondrial uncoupling protein 3 (UCP3) and hexokinase II (HKII) in primary rat skeletal muscle cells is dependent on reactive oxygen species. *Biochim. Biophys. Acta - Mol. Cell Res.* **1763**, 969–976.

Thelen, M. H., Simonides, W. S. and van Hardeveld, C. (1997). Electrical stimulation of C2C12 myotubes induces contractions and represses thyroid-hormone-dependent transcription of the fast-type sarcoplasmic-reticulum Ca2+-ATPase gene. *Biochem. J.* **321 (Pt 3)**, 845–8.

Untergasser, A., Cutcutache, I., Koressaar, T., Ye, J., Faircloth, B. C., Remm, M. and Rozen, S. G. (2012). Primer3--new capabilities and interfaces. *Nucleic Acids Res.* **40**, e115.

van Rooij, E., Liu, N. and Olson, E. N. (2008). MicroRNAs flex their muscles. *Trends Genet.* **24**, 159–66.

van Rooij, E., Quiat, D., Johnson, B. A., Sutherland, L. B., Qi, X., Richardson, J. A., Kelm, R. J. and Olson, E. N. (2009). A family of microRNAs encoded by myosin genes governs myosin expression and muscle performance. *Dev. Cell* **17**, 662–73.

Vélez, E. J., Lutfi, E., Jiménez-Amilburu, V., Riera-Codina, M., Capilla, E., Navarro, I. and Gutiérrez, J. (2014). IGF-I and amino acids effects through TOR signaling on proliferation and differentiation of gilthead sea bream cultured myocytes. *Gen. Comp. Endocrinol.* **205**, 296–304.

Vélez, E. J., Lutfi, E., Azizi, S., Montserrat, N., Riera-Codina, M., Capilla, E., Navarro, I. and Gutiérrez, J. (2016). Contribution of in vitro myocytes studies to understanding fish muscle physiology. *Comp. Biochem. Physiol. Part B Biochem. Mol. Biol.* **199**, 67–73.

von Hofsten, J., Elworthy, S., Gilchrist, M. J., Smith, J. C., Wardle, F. C. and Ingham, P. W. (2008). Prdm1- and Sox6-mediated transcriptional repression specifies muscle fibre type in the zebrafish embryo. *EMBO Rep.* **9**, 683–9.

Wang, X., Ono, Y., Tan, S. C., Chai, R. J., Parkin, C. and Ingham, P. W. (2011). Prdm1a and miR-499 act sequentially to restrict Sox6 activity to the fast-twitch muscle lineage in the zebrafish embryo. *Development* **138**, 4399–404.

Wickham, H. (2016). *Ggplot2 : elegant graphics for data analysis*. 2nd ed. (ed. Springer-Verlag) New York.

Yu, H., Lu, Y., Li, Z. and Wang, Q. (2014). microRNA-133: expression, function and therapeutic potential in muscle diseases and cancer. *Curr. Drug Targets* **15**, 817–28.

Figures

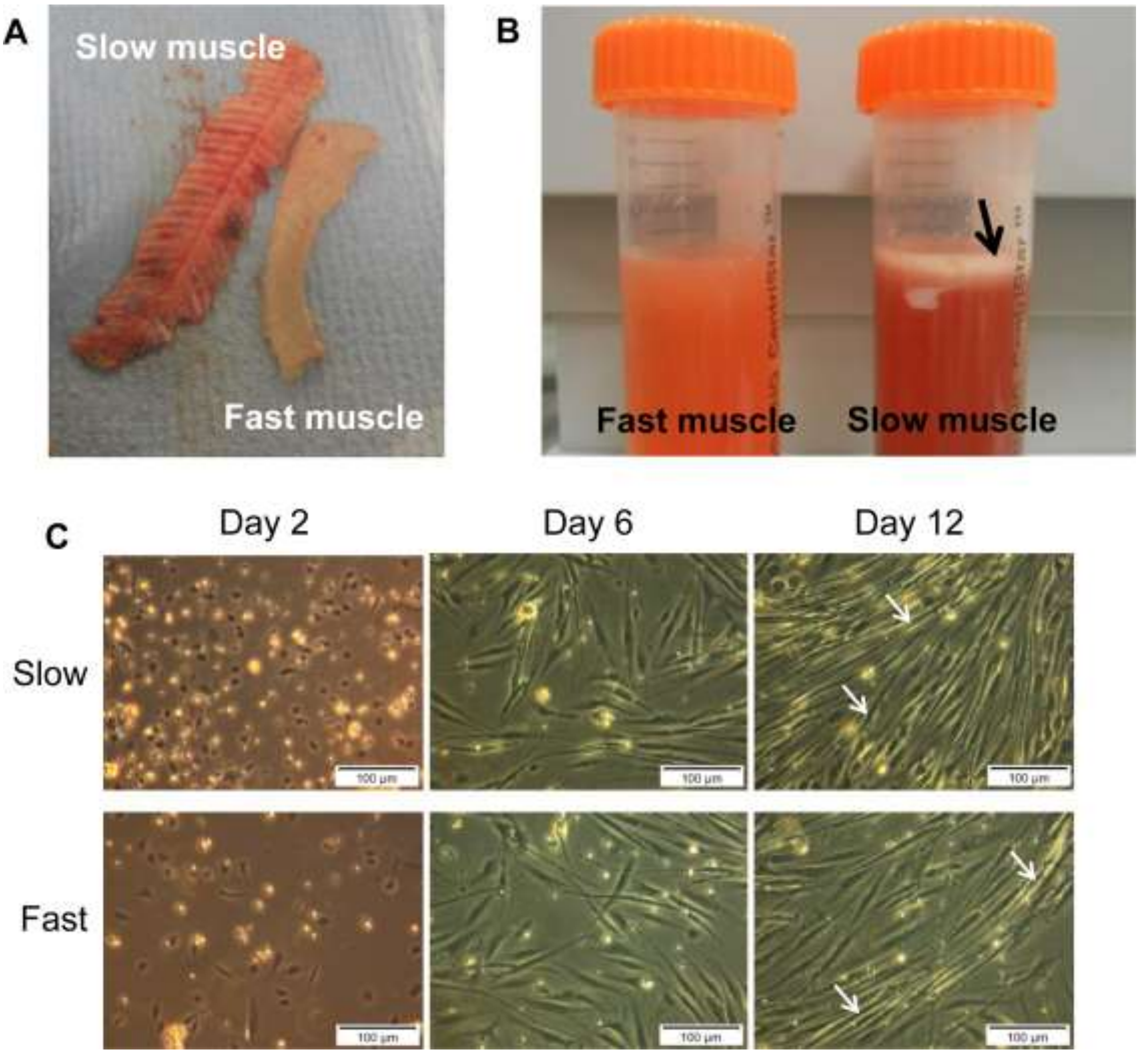

Fig. 1. Rainbow trout fast and slow myoblast cell culture establishment. (A) Slow muscle strips were carefully extracted from the surroundings of the lateral line and any remain of fast muscle was removed to avoid cross-contamination. Fast muscle samples were collected from the epaxial region after slow muscle removal. **(B)** Fast muscle extraction tube showing the DMEM media slightly orange due to pH reduction by lactic acid, and slow muscle extraction tube with a top layer of lipids (black arrow). **(C)** Rainbow trout fast and slow myoblasts at days 2, 6 and 12 of development (20x magnification). Myotubes indicated by white arrows.

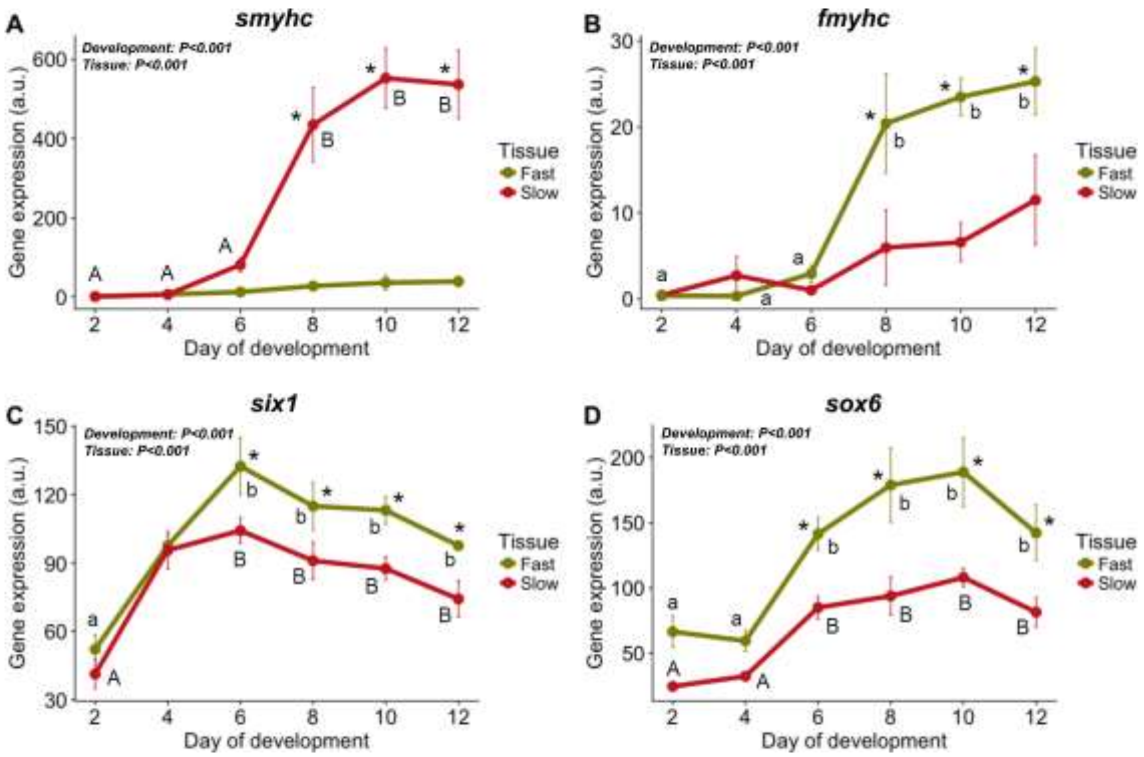

Fig. 2. Rainbow trout fast and slow myoblast cell culture characterization. Gene expression in slow and fast myoblast cell culture at days 2, 4, 6, 8, 10 and 12 of development for *slow myosin heavy chain* (*slow myhc*) **(A)**, *fast myosin heavy chain* (*fast myhc*) **(B)**, *six homeobox 1* (*six1*) **(C)** and *SRY (sex determining region Y) box 6* (*sox6*) **(D)**. Values represent mean ± SE (n=4 independent cell cultures; a.u.= arbitrary units). Data were analyzed using a two-way ANOVA followed by post hoc Tukey's honestly significant difference (HSD) test, with the tissue of origin (*tissue*) and the day of development (*development*) as factors. The P-values of *tissue* and *development* are shown in the left corner of each graph. Asterisks indicate significant differences between means of slow myoblasts and fast myoblasts cell cultures, and different letters (upper case for slow and lower case for fast) indicate significant differences between means of days of development ($P<0.05$).

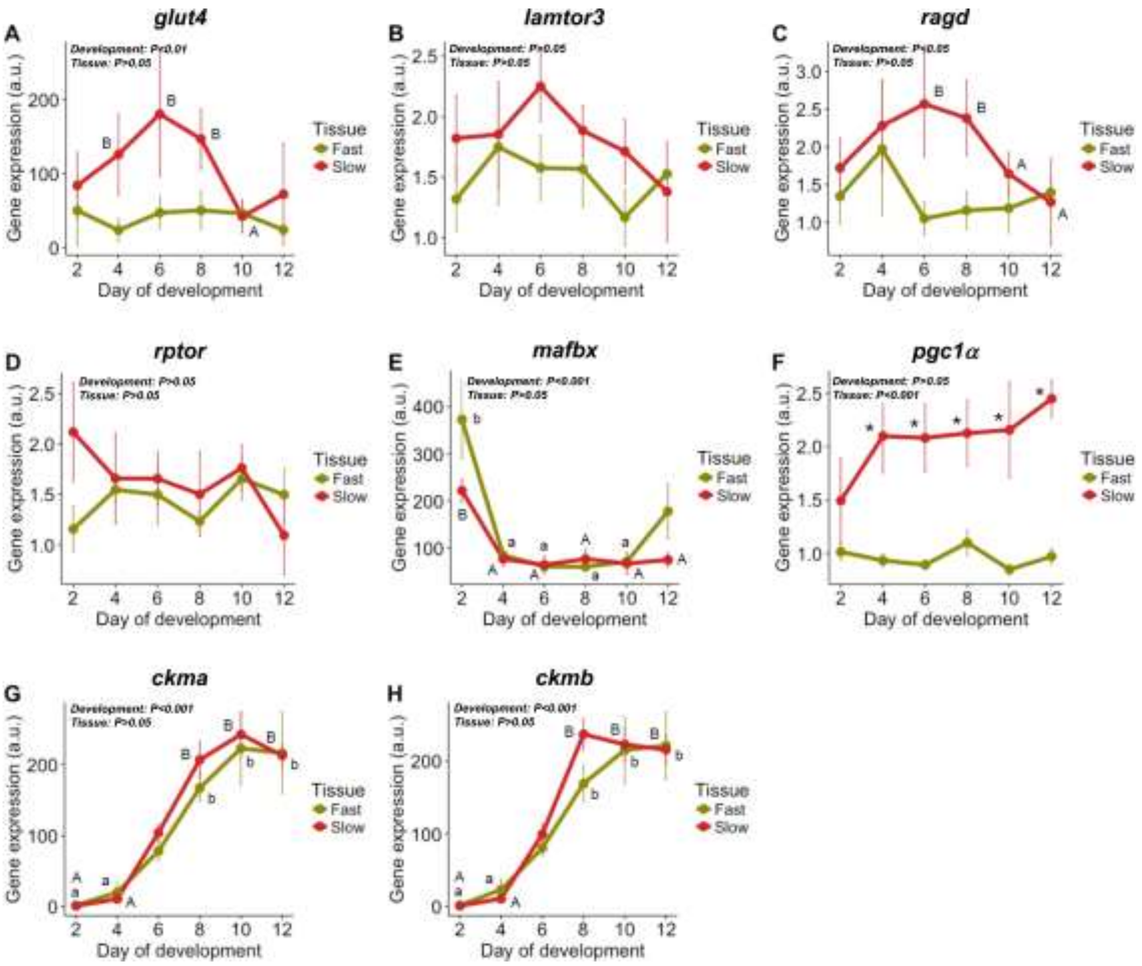

Fig. 3. Muscle regulatory signaling components in rainbow trout fast and slow myoblast cell culture. Gene expression in slow and fast myoblast cell culture at days 2, 4, 6, 8, 10 and 12 of development for *insulin-responsive glucose transporter type 4* (*glut4*) **(A)**, *late endosomal/lysosomal adaptor, mapk and mtor activator 3* (*lamtor3*) **(B)**, *ras related GTP binding D* (*ragd*) **(C)**, *regulatory associated protein of mtor complex 1* (*rptor*) **(D)**, *muscle atrophy f-box protein* (*mafbx*) **(E)**, *peroxisome proliferator-activated receptor gamma coactivator 1 alpha* (*pgc1α*) **(F)**, *creatine kinase, m-type a* (*ckma*) **(G)** and *creatine kinase, m-type b* (*ckmb*) **(H)**. Values represent mean ± SE (n=4 independent cell cultures; a.u.= arbitrary units). Data were analyzed using a two-way ANOVA followed by post hoc Tukey's honestly significant difference (HSD) test, with the tissue of origin (*tissue*) and the day of development (*development*) as factors. The P-values of *tissue* and *development* are shown in the left corner of each graph. Asterisks indicate significant differences between means of slow myoblasts and fast myoblasts cell cultures, and different letters (upper case for slow and lower case for fast) indicate significant differences between means of days of development (P<0.05).

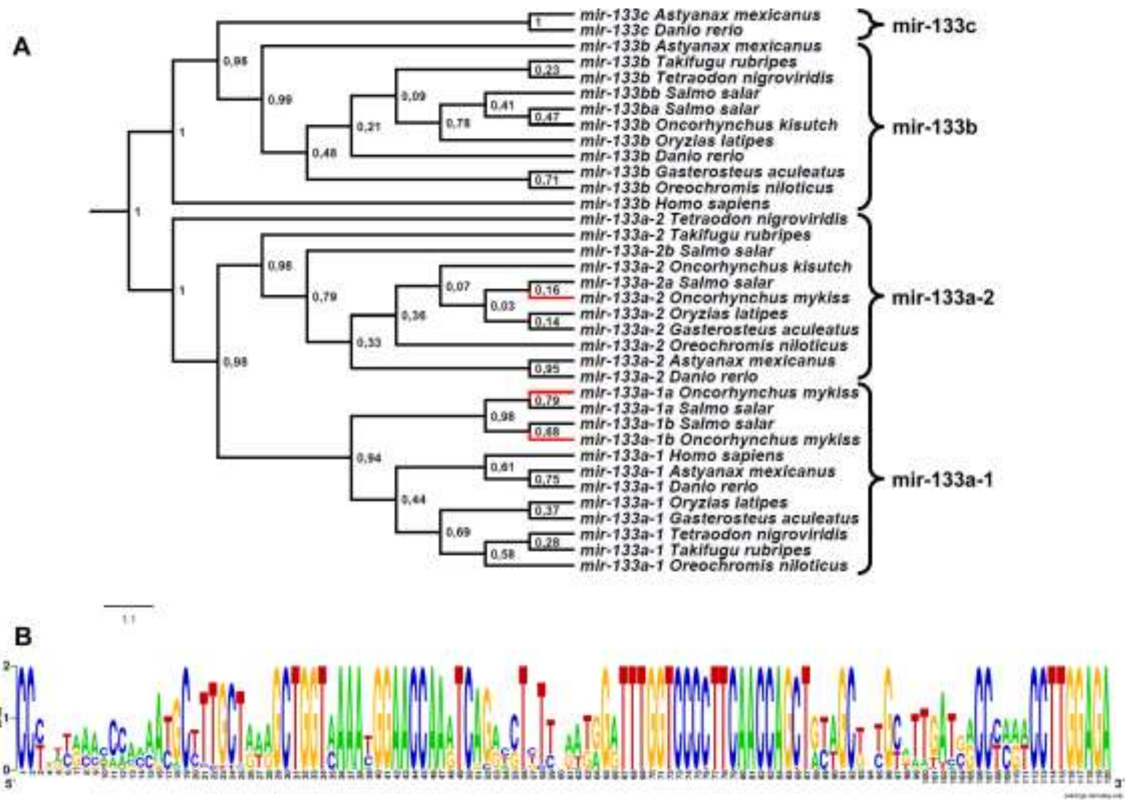

Fig. 4. Teleost fish *mir-133* phylogenetic analysis. (A) Phylogenetic reconstruction of the *mir-133* family using Bayesian methods. The tree was constructed from a high confidence alignment of 36 pre-miRNA sequences and used Hasegawa-Kishino-Yano with Gamma distribution (HKY+G) as the best fitted substitution model. Bootstrap-posterior values are indicated on the node of each branch. Branches in red indicate the *mir-133* copies identified for rainbow trout. **(B)** Multiple alignment was analyzed on WebLogo 3 server from University of California, Berkeley for logo representation of all the miRNAs used for the phylogenetic reconstruction; the Y-axis represents conservation of nucleotides at that position (height).

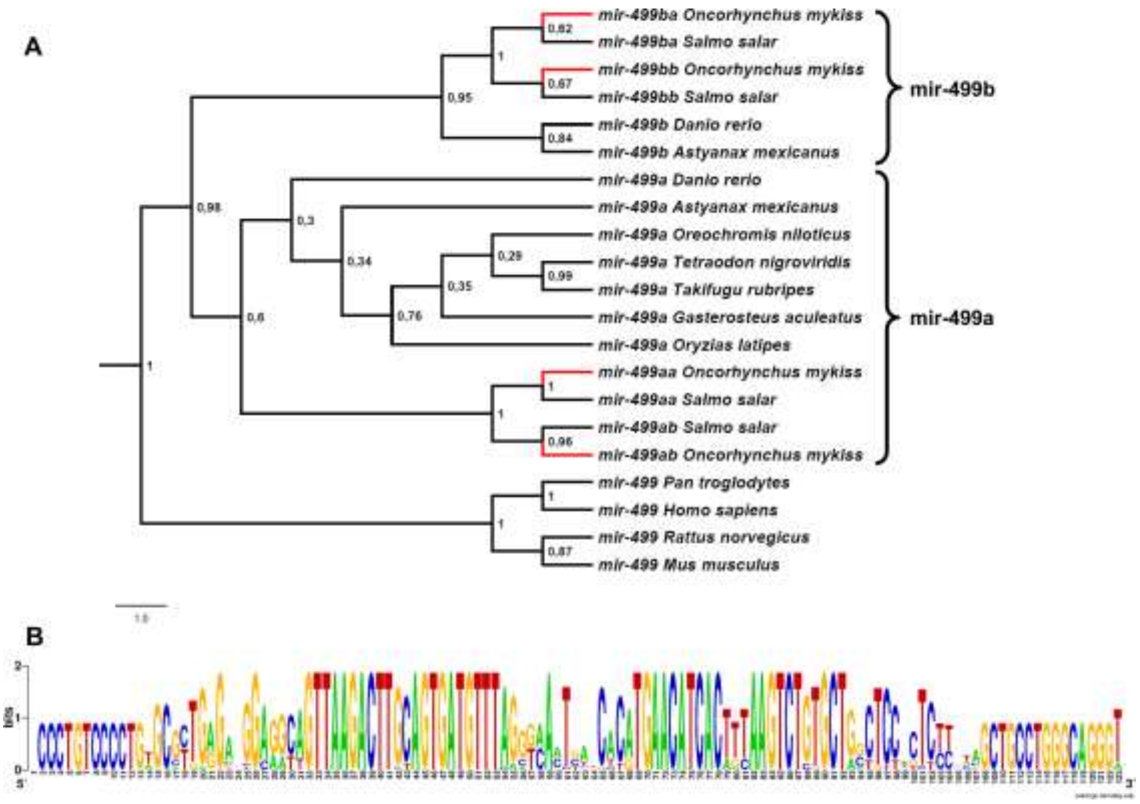

Fig. 5. Teleost fish *mir-499* phylogenetic analysis. (A) Phylogenetic reconstruction of the *mir-499* family using Bayesian methods. The tree was constructed from a high confidence alignment of 21 pre-miRNA sequences and used Hasegawa-Kishino-Yano with Gamma distribution (HKY+G) as the best fitted substitution model. Bootstrap-posterior values are indicated on the node of each branch. Branches in red indicate the *mir-499* copies identified for rainbow trout. **(B)** Multiple alignment was analyzed on WebLogo 3 server from University of California, Berkeley for logo representation of all the miRNAs used for the phylogenetic reconstruction; the Y-axis represents conservation of nucleotides at that position (height).

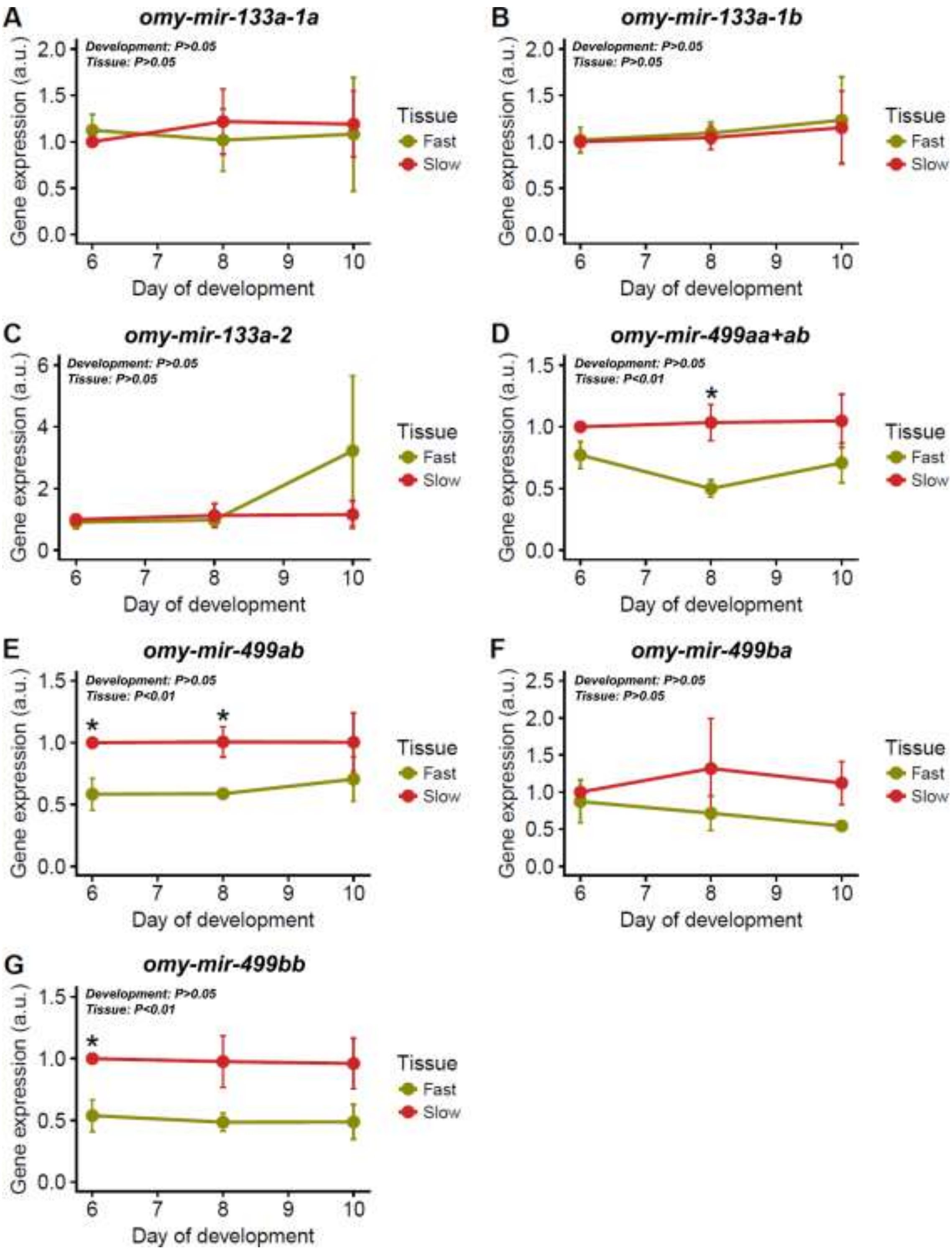

Fig. 6. *miR-133* and *miR-499* paralogue expression in rainbow trout fast and slow myoblast cell culture. Gene expression in slow and fast myoblast cell culture at days 6, 8 and 10 of development for *omy-mir-133a-1a* **(A)**, *omy-mir-133a-1b* **(B)**, *omy-mir-133a-2* **(C)**, *omy-mir-499aa+ab* **(D)**, *omy-mir-499ab* **(E)**, *omy-mir-499ba* **(F)** and *omy-mir-499bb* **(G)**. Values represent mean ± SE (n=4 independent cell cultures; a.u.=

arbitrary units). Data were analyzed using the unpaired t-test with the tissue of origin (*tissue*) as factor. The P-values of the *tissue* and the day of development (*development*) are shown in the left corner of each graph. Asterisks indicate significant differences between means of slow myoblasts and fast myoblasts cell cultures ($P<0.05$).

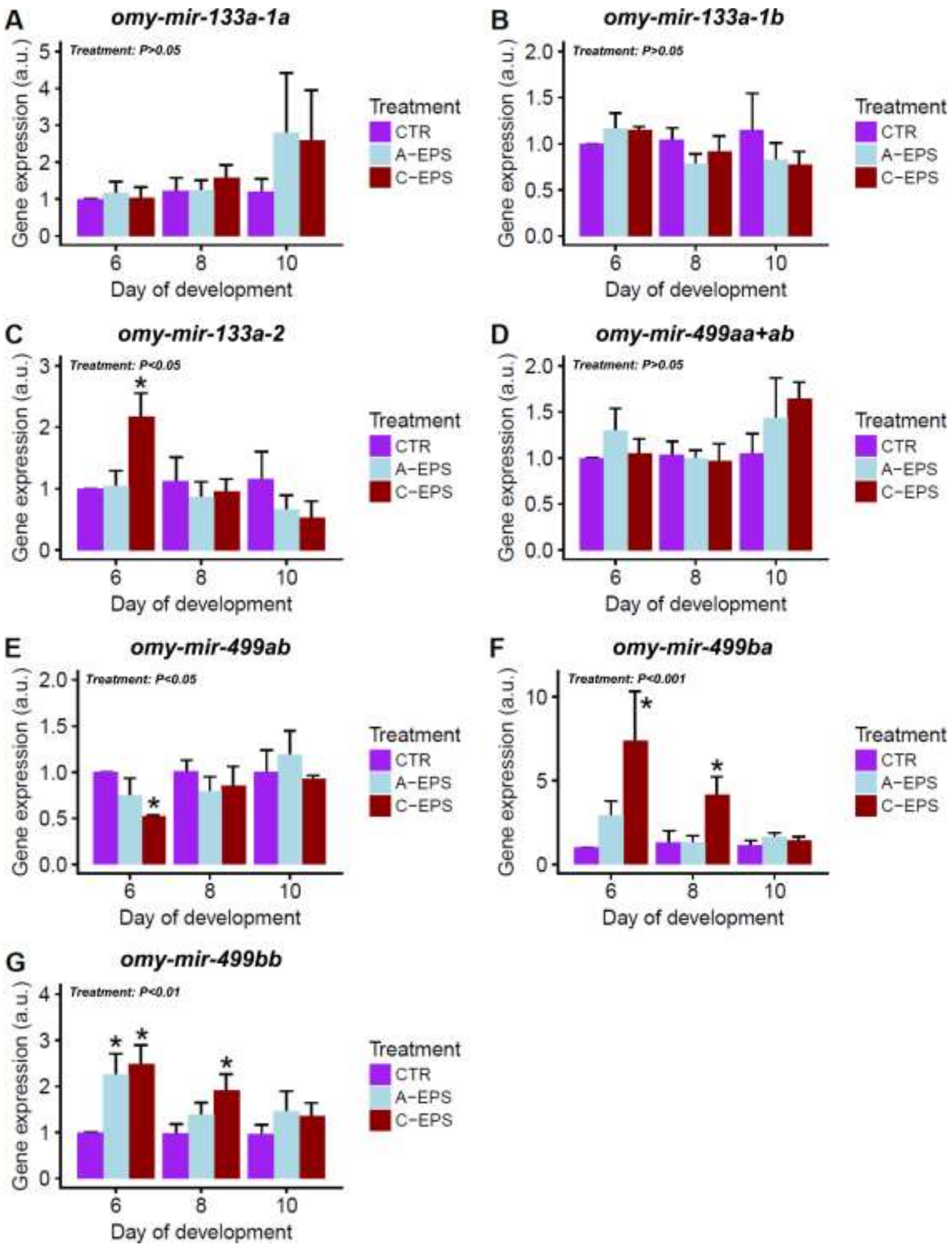

Fig. 7. ***miR-133*** **and** ***miR-499*** **paralogue expression in rainbow trout slow myoblast cell culture treated with electrical pulse stimulation (EPS).** Gene expression in slow myoblast cell culture at days 6, 8 and 10 of development for *omy-mir-133a-1a* **(A)**, *omy-mir-133a-1b* **(B)**, *omy-mir-133a-2* **(C)**, *omy-mir-499aa+ab* **(D)**, *omy-mir-499ab*

(E), *omy-mir-499ba* **(F)** and *omy-mir-499bb* **(G)**. The treatments are as follow: non-treated myoblasts (CTR, purple bar); myoblasts submitted to acute and high-frequency stimulation (A-EPS, blue bar); and myoblasts submitted to chronic and low-frequency stimulation (C-EPS, red bar). Values represent mean ± SE (n=4 independent cell cultures; a.u.= arbitrary units). Data were analyzed using a one-way ANOVA followed by post hoc Dunn's test, with the EPS treatment (*treatment*) as factor. The P-values of *treatment* are shown in the left corner of each graph. Asterisks indicate significant differences between means of EPS treatments compared to CTR ($P<0.05$).

Table S1: Precursor miRNA sequences of each species used in the analyses and their respective nomenclature according to the evolutionary relationship provided by the Bayesian phylogenetic trees.

Click here to Download Table S1

Table S2: Quantitative PCR primer sequences. Genes are as follow: *slow myhc* (*slow myosin heavy chain*); *fast myhc* (*fast myosin heavy chain*); *sox6* ((*sex determining region Y*)-*box 6*); *six1* (*six homeobox 1*); *glut4* (*insulin-responsive glucose transporter type 4*); *lamtor3* (*late endosomal/lysosomal adaptor, mapk and mtor activator 3*); *ragd* (*ras related GTP binding D*); *rptor* (*regulatory associated protein of mtor complex 1*); *mafbx* (*muscle atrophy f-box protein*); *pgc1α* (*peroxisome proliferator-activated receptor gamma coactivator 1 alpha*); *ckma* (*creatine kinase, m-type a*); *ckmb* (*creatine kinase, m-type b*); *myog* (*myogenin*); *rpl13* (*ribosomal protein L13*); *rpl19* (*ribosomal protein L19*); *omy-mir-133a-1a*, *omy-mir-133a-1b*, *omy-mir- 133a-2* (precursor sequences of rainbow trout mir-133 paralogues); *omy-mir-499aa+ab*, *omy-mir-499ab*, *omy-mir-499ba*, *omy-mir-499bb* (precursor sequences of rainbow trout mir-499 paralogues); *omy-mir-206-1* (precursor sequence of rainbow trout mir-206); and *U6 snRNA* (*U6 small nuclear RNA*). Accession code based on rainbow trout genome in Genoscope (https://www.genoscope.cns.fr/trout/) (Berthelot et al., 2014) or NCBI (http://www.ncbi.nlm.nih.gov) database.

Gene	Primers (5' to 3')	Tm (°C)	Accession code
slow myhc	F: AGTTCCGCAAGATTCAGCAT R: GCCGACATCACAACTCTTGA	81	AF211172.1
fast myhc	F: GGCCAAGAAGGCTATCACTG R: GCCAGATTCTCAGCCTCATC	84	Z48794.1
sox6	F: TGGGAGAGGATGATGGAAAG R: CCCAGGATCTTGCTGATGTT	85	XM_021566535.1
six1	F: TCCCTCTGGATATCGGCGTT R: AGAAAACGACCGAGCCTCTC	83	XM_021574266.1
glut4	F: GTGCCAGGCTTATTGTCCATATTC R: TAGAGAAGATGGCCACCGACAG	85	XM_021615262.1
lamtor3	F: TCACCATGGACTGGGGGTTA R: TGCGTTATCATTTGCCACTTTG	79	NM_001160681.1
ragd	F: AGGGGGTTTCGAAGTACACC R: TGAAACCACCTCCGTCTTCG	80	XM_021573884.1
rptor	F: CCATCGACAAGATGAGACGA R: CCTGGGGAGACAGAGACAGA	86	XM_021557184.1
mafbx	F: CAGGAGCCCGAGTGACTTTT R: ATCAAATGCACCATCACCCCT	76	NM_001193326.1
pgc1α	F: AACCTGAGAGATGACGGGGA R: GTGTGTCCGTTTTCAAGGGC	78	XM_021617116.1
ckma	F: GTGGGTGGAGTGTTCGACAT R: TCCACCATGAGCTTGACACC	82	XM_021623857.1
ckmb	F: AGCACACACCCCAAGTTTGA R: CAGAAGATCCCAGACGGTCA	84	XM_021617754.1

myog	F: AGCAACACCTCAGACCACTG R: AGGAGGTCCTCGTTGCTGTA	75	NM_001124727.1
rpl13	F: CACCATTGGCATCTCTGTTG R: AGTGCTGTCTCCCTTCTTGG	85	scaffold_1560 chrUn_26:11288161..11308160
rpl19	F: GAGAAGACGACGCAGGATTC R: CAAGTGAAGGCACACAGGAA	80	scaffold_1008 chrUn_1:27789918..27809917
omy-mir-133a-1a	F: AGTGAACCCCCAATGCTTT R: GGGACCAAATCCATTCAAGA	73	scaffold_1560 chrUn:390576274..390581273
omy-mir-133a-1b	F: GACAAACACCTAATGCCTTG R: GGGACCAAATCCATTCAAGA	73	scaffold_79929 chrUn:366226605..366231604
omy-mir-133a-2	F: TTCACACCAAAAATGCTTT R: GGGACCAAATCCATTGAACA	71	scaffold_1154 chrUn:346363877..346368876
omy-mir-499aa+ab	F: CTGAGAAGGAGACAGTTAAGACTTG R: AGAGTGGAGCCAGCAGAGAC	74	scaffold_984 chrUn_17:42432554..42452553
omy-mir-499ab	F: AGGAGACAGTTAAGACTTGC R: TGAGAATGGAGCCAGCAC	74	scaffold_116 chrUn_7:18225955..18230954
omy-mir-499ba	F: GAGGGAAGTAGTTAAGACTTG R: CTTAAAGTGATGTTCATGAGT	70	scaffold_347 chrUn_9:20331061..20336060
omy-mir-499bb	F: GAGGGAAGTAGTTAAGACTTA R: CTTAAAGTGATGTTCATGAGC	70	scaffold_1915 chrUn_16:304245..309244
omy-mir-206-1	F: TCGTTGCCTCCTGTGAAGAC R: CTCCATTCCCCTTGTAACCA	76	scaffold_13810 chrUn:893645720..893645918
U6 snRNA	F: GGCTTCGGCAGCACATATAC R: AACGCTTCACGATTTTGC	77	scaffold_15039 chrUn:278113300..278133299

Tm, melting temperature; F, forward; R, reverse.

Table S3: Rainbow trout miRNAs similarity. Percentage of similarity between miRNAs paralogues identified in rainbow trout.

Paralogue	Nucleotide similarity
omy-mir-133a-1a vs *omy-mir-133a-1b*	97%
omy-mir-133a-1a vs *omy-mir-133a-2*	93%
omy-mir-133a-1b vs *omy-mir-133a-2*	92%
omy-mir-499aa vs *omy-mir-499ab*	96%
omy-mir-499ba vs *omy-mir-499bb*	97%

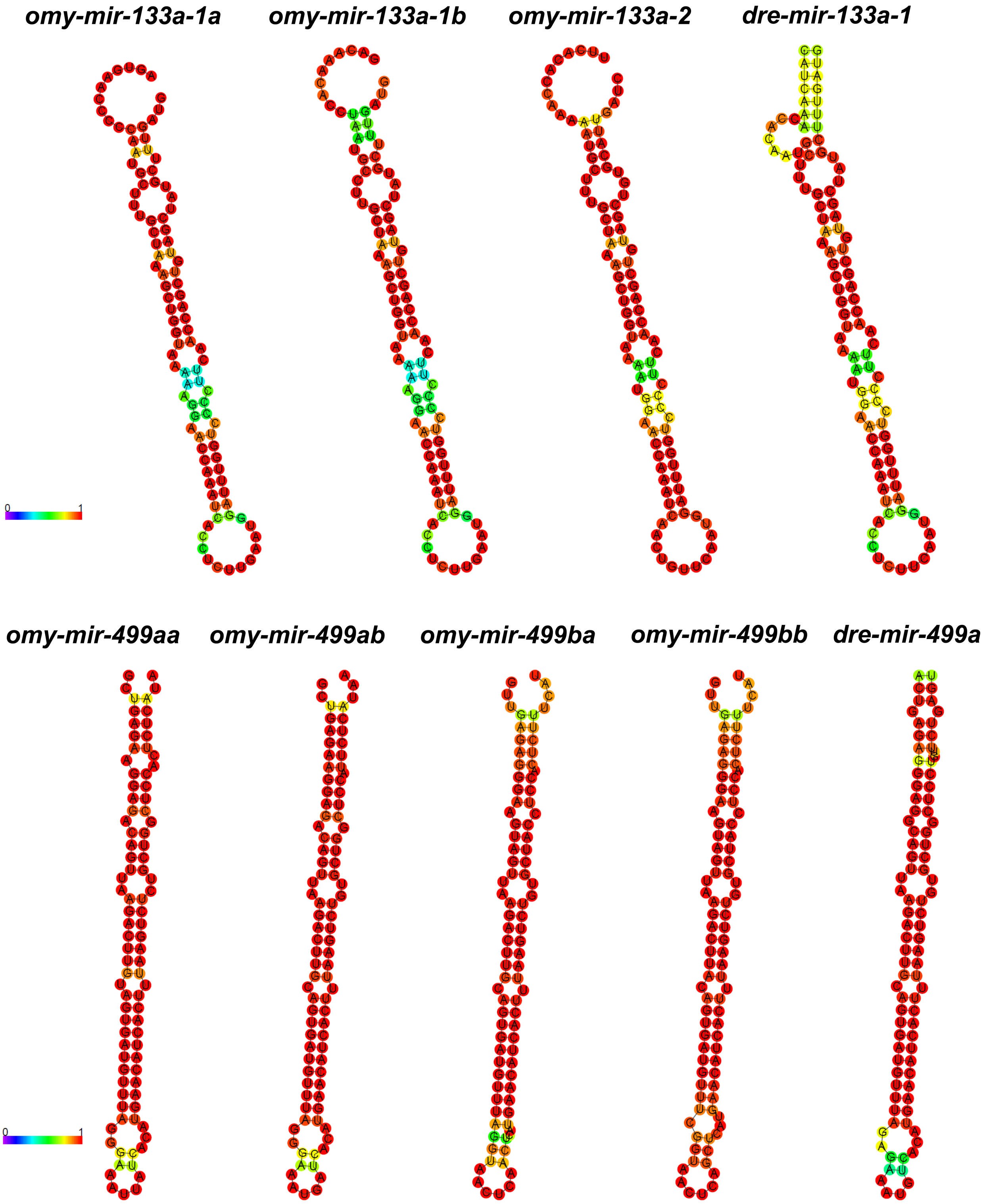

Figure S1: Predicted secondary structures of the identified miRNA precursor sequences. The precursor sequences of the mir-133 and mir-499 paralogues were submitted to minimum free energy (MFE) prediction of the optimal secondary structures in dot-bracket notation. Base pair probabilities are color coded 0-1, with higher numbers corresponding to higher confidence. Secondary structures of zebrafish *dre-mir-133a-1* and *dre-mir-499a* precursor sequences are shown only for comparative purposes.

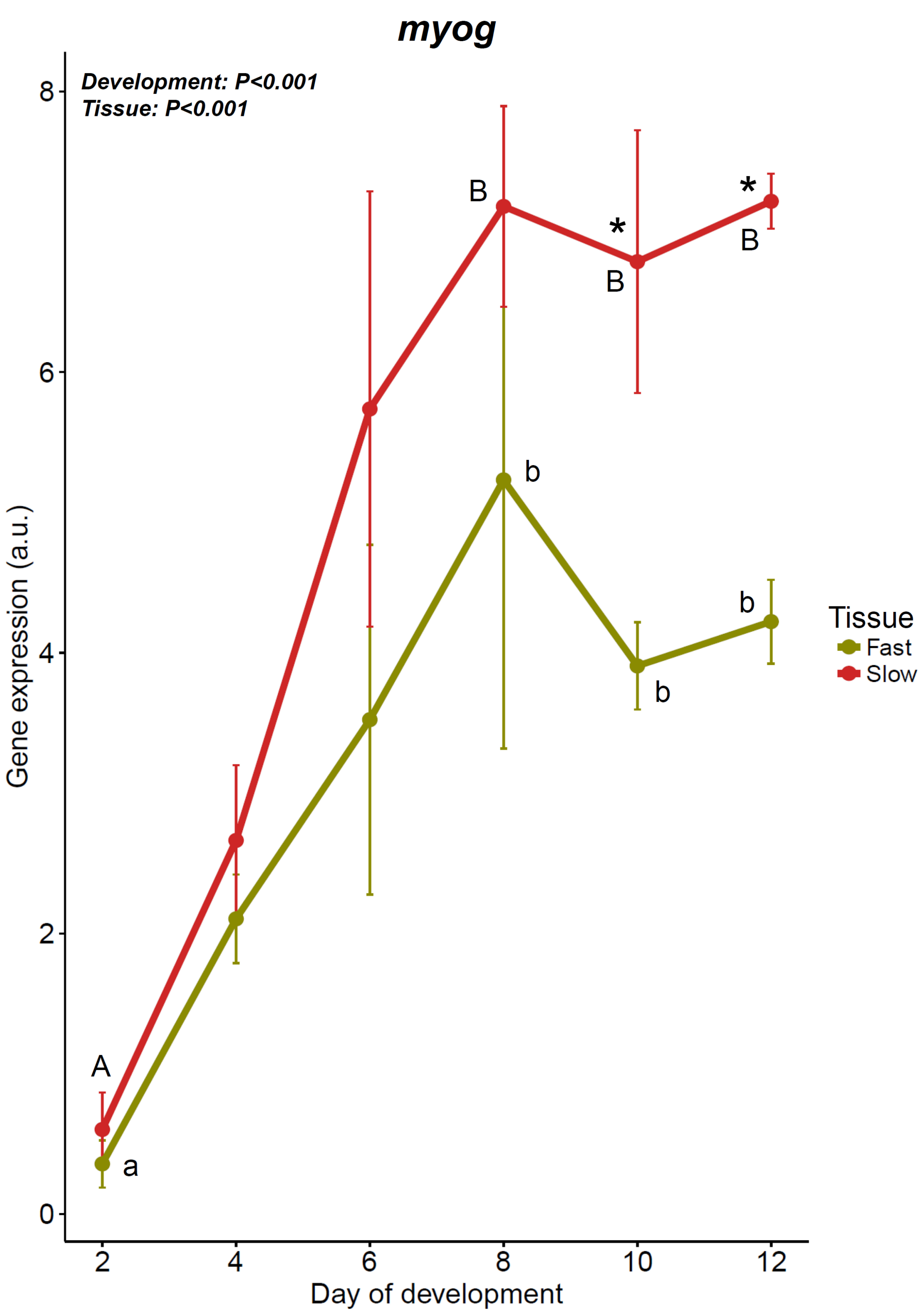

Figure S2: *Myogenin* expression in rainbow trout fast and slow myoblast cell culture.

Myogenin (*myog*) expression in slow and fast myoblast cell culture at days 2, 4, 6, 8, 10 and 12 of development. Values represent mean ± SE (n=4 independent cell cultures; a.u.= arbitrary units). The P-values of the tissue of origin (*tissue*) and the day of development (*development*) are shown in the left corner of the graph. Asterisks indicate significant differences between means of slow myoblasts and fast myoblasts cell cultures, and different letters (upper case for slow and lower case for fast) indicate significant differences between means of days of development (P<0.05).

A

Correlation	133a1a	133a1b	133a2	499aa +ab	499ab	499ba	499bb	*smyhc*	*fmyhc*	*sox6*
133a1a	1	0,21	0,11	0,2	0,12	0,02	0,17	-0,12	-0,02	0,26
133a1b		1	0,55***	-0,1	0,16	0,14	0,09	-0,2	0,55***	0,4**
133a2			1	-0,1	-0,05	0,27	0,21	0,02	0,26	0,13
499aa+ab				1	0,71***	0,11	0,6***	0,26	-0,17	-0,38*
499ab					1	0,13	0,41**	0,46**	0,21	-0,27
499ba						1	0,69***	0,15	-0,24	-0,5**
499bb							1	0,08	-0,31*	-0,51***
smyhc								1	0,19	-0,46**
fmyhc									1	0,45**
sox6										1

B

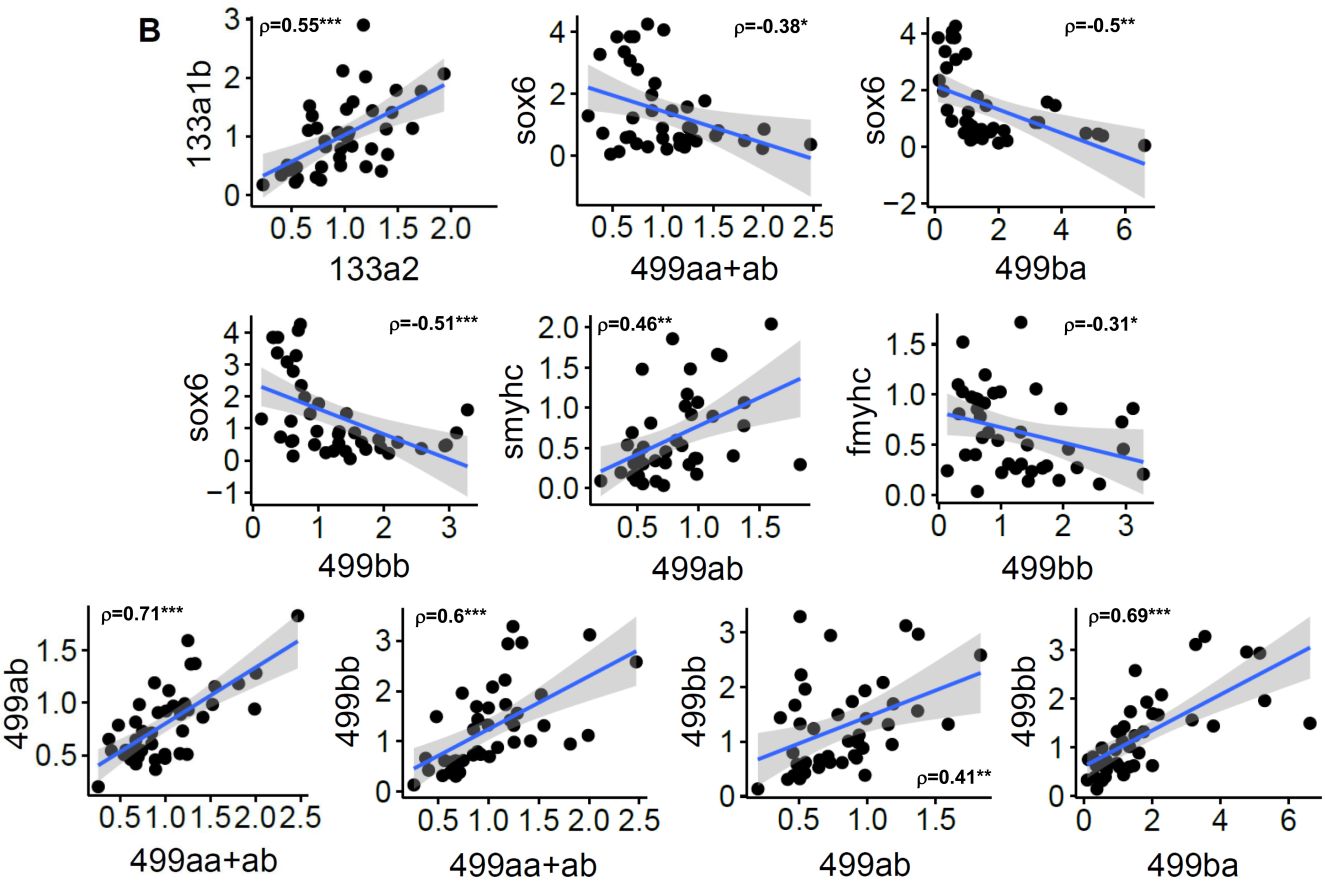

Figure S3: Correlation of rainbow trout miRNAs and mRNAs expression. (A) Pearson's correlation (ρ) index between the expression of *omy-mir-133* and *omy-mir-499* paralogues, and *smyhc*, *fmyhc* and *sox6* mRNAs. (B) Plot char between gene expression values for *omy-mir-133a-1b* vs *omy-mir-133a-2*, *omy-mir-499aa+ab* vs *sox6*, *omy-mir-499ba* vs *sox6*, *omy-mir-499bb* vs *sox6*, *omy-mir-499ab* vs *smyhc*, *omy-mir-499bb* vs *fmyhc*, *omy-mir-499aa+ab* vs *omy-mir-499ab*, *omy-mir-499aa+ab* vs *omy-mir-499bb*, *omy-mir-499ab* vs *omy-mir-499bb* and *omy-mir-499ba* vs *omy-mir-499bb*. Pearson correlation and p-value are indicated in the corners of the plot graphs. Significant differences between gene correlations are indicated with one (P<0.05), two (P<0.01) or three (P<0.001) asterisks.